Electrical conduction through single molecules and self-assembled monolayers

TOPICAL REVIEW

Electrical conduction through single molecules and self-assembled monolayers

Hylke B Akkerman and Bert de Boer

Zernike Institute for Advanced Materials, University of Groningen, Nijenborg 4, NL-9747 AG,
Groningen, The Netherlands

E-mail: b.de.boer@rug.nl

Abstract
Although research on molecular electronics has drawn increasingly more attention in the last
decade, the large spread in obtained results for the conduction rescaled to a single molecule
indicates a strong dependence of the measured data on the experimental testbed used. We
subdivided a generalized metal–molecule–metal junction into different components and discuss
their influence on electrical transport measurements of a single organic molecule or an assembly
of molecules. By relating the advantages and disadvantages of different experimental testbeds
to the more general view of a molecular junction, we strive to explain the discrepancies between
the obtained results on molecular conduction. The reported results on molecular conduction of
molecules with an alkane backbone can be categorized into three groups with different
resistance values, depending on the device area of the molecular junction and the nature of the
contacts.

Contents

1. Introduction

In 1960 Herwald and Angello published an article in *Science* stating that 'The trend in electronics circuit construction is toward microminiaturization and molecular electronics.' [1]. In this article they envisioned that 'the boundaries between materials and devices and between devices and circuits are being removed, and we shall see an integration of disciplines in the future development of molecular electronics.' Although the term *molecular electronics* was at that time used interchangeably with integrated circuits and semiconductor networks, the question remains whether they still might be proven right when the term 'molecular electronics' is used with its present-day meaning, i.e., electronic components based on a single molecule or an assembly of molecules. Since 1965, when Gordon E Moore made his famous observation that the number of transistors on an integrated circuit increases exponential in time [2], known as Moore's Law, technological development has proven to keep up with this prophetic observation. The initial prediction was a doubling of the

number of transistors every year, but later Moore adjusted this to every 2 years. Although it remains unclear when the end of Moore's Law is reached with current silicon-based technology and whether it will lead to serious problems for technological development, molecular electronics is often proposed as a candidate to overcome the possible downscaling limitation in silicon. In 1974, Aviram and Ratner proposed a method of making a rectifier based on a single organic molecule [3]. The concept of making a functional device, based on the properties of a single molecule offers, in theory, unlimited possibilities for technological development, since the electrical properties of organic molecules can be altered by molecular design and synthesis. Furthermore, by using 2-terminal devices with a single organic molecule, the inevitable downscaling limit in silicon integrated circuits might be overcome and Moore's Law would continue to thrive for the coming decades. The decrease in lateral size is only one of many development requirements for transistors on silicon chips. Operation speed, reliability, stability, power consumption and, perhaps most important, production costs are all critical for an emerging technology that is intended to compete with or follow-up silicon-based technology. There is no evidence so far that electronic components based on organic molecules can compete with silicon on all these requirements, especially operation speed. When molecular electronics cannot live up to these requirements, perhaps the future of molecular electronics is in low end applications. In low end applications the operation requirements are less critical, but processing costs should be as low as possible. Instead of using single molecules to provide the electronic functionality, self-assembled monolayers (SAMs) might be used, where the functionality is still incorporated in the molecular structure but an assembly of molecules is used. SAMs are formed by molecules in solution which attach themselves with an end group to a specific substrate to form a densely packed molecular monolayer. The name *self-assembled monolayers* already explains the low production costs, the molecules assemble themselves at the designated surface or electrode, without any external influences. Furthermore, the costs are low since only small quantities are required to cover large areas, making self-assembled monolayers a very inexpensive primary product. For example, with only 1 g of dodecanethiol molecules (HS-$C_{12}H_{25}$), a densely packed SAM on gold can be formed over an area of ∼600 m^2. Whether molecular electronics will be used in the next generation computer chips or whether it will provide the future for low end applications, only time will tell. No matter what direction the future will hold for molecular electronics, it is certainly worth developing this emerging technology for future applications and, perhaps even more interesting, fundamental scientific understanding.

Research on molecular electronics has drawn increasingly more attention since the last decade (figure 1), but the first electrical measurements on SAMs were already performed as early as 1971, by Mann and Kuhn [4]. They fabricated monolayers of fatty acid salts, $(CH_3(CH_2)_{n-2}COO)_2Cd$, of different chain lengths with $n = 18–22$. These monolayers were formed on Al electrodes and mercury was used to fabricate the top electrode. Although, lacking sophisticated
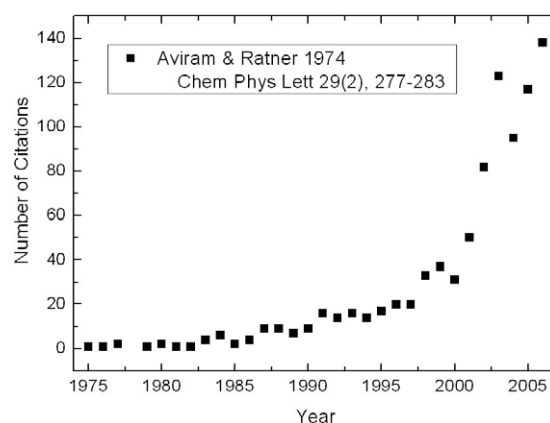

Figure 1. The number of citations each year to the seminal article by Aviram and Ratner published in 1974 ([3]), proposing a rectifier based on a single organic molecule. The last decade shows a tremendous increase in the number of citations, clearly indicating a strong growth in attention for molecular electronics [5].

fabrication techniques such as photolithography, they still managed to obtain an exponential decrease in the current with increasing molecule length, i.e., layer thickness of the insulating barrier, clearly demonstrating the tunneling nature of the electron current through these SAMs.

For the development of every emerging technology, the fundamental principles underlying this technology need to be understood before significant progress can be made in the field. For exactly that reason alkane-based molecules, as were used by Mann and Kuhn, are a perfect benchmark for any new experimental testbed in molecular electronics. SAMs of alkane(di)thiols are known to form densely packed and well-ordered mono-domains up to several hundred square nanometers on gold [6–8]. Comprising an alkane backbone and either one thiol end group (monothiol) for anchoring the molecule to Au, or a thiol at both ends of the alkane chain (dithiol), these molecules can easily be varied in length by varying the number of carbon atoms in the alkane chain. Since alkane(di)thiols possess a large energy gap between the highest occupied molecular orbital (HOMO) and lowest unoccupied molecular orbital (LUMO) of about 8–10 eV [9, 10], these molecules are insulating and, consequently, a tunneling current is expected which decreases exponential with increasing molecule length and is temperature independent. This property allows for a solid verification whether or not the properties of the molecules under study are indeed measured. Since the first measurements on alkane-based SAMs were already performed more than 3 decades ago [4] and the alkane-based molecules make an ideal benchmark for molecular electronics, we might expect that the electrical properties of alkanes are already fully understood. This is, unfortunately, not the case. A large spread in conduction per molecule is obtained for these types of molecules for different molecular junction geometries or molecular electronics testbeds [10, 11]. The differences in conduction per molecule vary up to 8 orders of magnitude. The true cause behind this large spread in results still remains unclear and is subjected to analysis at the end of this review.

Nevertheless, alkane(di)thiol molecules can be considered as a perfect benchmark for any new technology related to
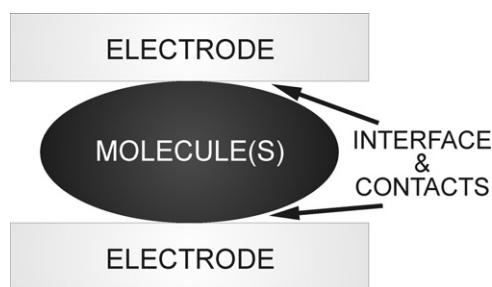
Figure 2. Schematic representation of a molecular junction. One or more molecules are sandwiched between two electrodes.

molecular electronics since the exponential length dependence and temperature independence are the well-defined electrical characteristics of the tunneling current, which can be measured. However, the large spread in absolute value for the conduction per molecule from different experiments makes it extremely hard to relate the experiments to theory [12–15]. Therefore, we investigate in this review the different experimental testbeds used and compare the obtained results on alkane(di)thiols after a thorough analysis of the different aspects of each measurement set-up. This provides not only an overview of the current status of the field, but hopefully also delivers a clear insight in the cause behind the variations in the obtained results.

2. Molecular junctions in general

To analyze the different testbeds used in molecular electronics, we first need to generalize and simplify a molecular junction to obtain the different elements of the junction, which are influencing or even critical for the electrical measurements. A schematic drawing of a molecular junction is shown in figure 2, where one or more molecules are sandwiched between two electrodes. The junction can be divided into 3 major regions, i.e., the electrodes, the molecule(s) and the interfaces between each contact and the molecules.

2.1. The electrodes

Except for the break junction techniques, all other types of molecular junctions do not have both electrodes fabricated simultaneously. First, one electrode is fabricated, then a SAM is formed on this electrode, and the final step involves the formation of a second electrode. Depending on the atomic structure of the type of substrate/metal used, SAMs can form with differences in packing density and tilt angle [7, 16]. Since the molecules are typically about 2 nm in length, the surface topography and roughness of the electrodes are strongly determining the final configuration of the junction, and thus the observed electrical characteristics of the molecular junction [17–22]. The local contact geometries in nanoscale junctions for single molecule measurements are never identical. Therefore, statistics need to be done on a large collection of measurements to average out these geometrical variations [23–30]. For larger junctions, where large assemblies of molecules are measured simultaneously, contact

geometries will also never be identical. However, due to the large collection of different local geometries in one junction, the large scale junctions result in an average conduction value [31]. Consequently, single molecule experiments and measurements on SAMs result often in different conductance values [10, 11, 32]. The exact dimensions of these electrodes or the device area are important in combination with the metal type (Au, Ag, Pt, Pd, Hg, GaAs, etc) and roughness, to determine accurately the number of molecules in the junction. Another obvious requirement for a well-defined bottom electrode is the cleanness of its surface. Thiols cannot attach themselves easily on polluted gold surfaces, it requires a significantly longer time or they do not assemble at all. Thiols are most likely able to displace any adsorbates at the surface [7], but to ensure a well-defined system, adsorbates at the electrode surface must be avoided.

The second or top electrode is perhaps even more critical than the bottom electrode. Evaporating metals on top of SAMs results likely in filamentary growth of the metal atoms through the SAM, introducing short circuits [33–35]. Therefore, evaporating metals directly on SAMs results in a very low yield of working devices [36] and results will be unreliable and irreproducible when only few devices are fabricated. Top electrodes that do not create short circuits need to be well defined and reproducible. The majority of the wide range of experimental testbeds discussed in this review can be subdivided based on their top contact and the method of applying this top contact.

2.2. The molecules

Any kind of molecule used in molecular electronics can be divided into three parts:

(1) The surface-active head group that anchors the molecule to the first electrode,
(2) The backbone of the molecule, and
(3) The functional end group that might contain the proper functionality to ensure a good contact to the top electrode [7, 37, 38].

The molecules studied can vary in length, composition, orientation and packing. In this review, however, we limit ourselves to studies on alkane(di)thiols. Alkanedithiols, just as alkanemonothiols, are also known to appear in different phases; a flat phase with the molecules parallel to the surface [39], a standing-up phase with only one thiol bonded to gold, a looped phase with both thiols attached or a combination of both looped and standing-up molecules [40, 41]. The flat lying molecules most likely form when they are assembled from the gas phase or in solution at extremely low concentrations. The looped and standing-up phases appear when the alkanedithiol monolayers are assembled from a low concentrated solution and a highly concentrated solution, respectively. Several aspects during the self-assembly will affect the final phases formed, namely:

(1) Increasing the chain length will enhance the possibility for the alkanedithiols to loop back to the surface [40, 41].

(2) The use of different solvents or solvent mixtures can play a decisive role in the formation of the final phase on the surface [42, 43].

(3) The kind of metal or semiconductor surface used [7, 16, 22].

(4) The temperature during the self-assembly [41, 44].

(5) The optional addition (and concentration) of deprotection agents when thioacetyl groups are utilized [45].

Clearly, different phases might lead to significant changes in conduction [19, 41].

2.3. The molecule–electrode interface

The interface or the contact between the molecules and the electrodes can be a chemisorbed or physisorbed contact [7]. For a chemisorbed contact, the end group of the molecule is chemically bonded to the electrode. Although the formation is not fully understood yet, the Au–S bond is known to be a chemisorbed contact [7, 8, 46, 47]. The difference between a chemisorbed contact and a physical contact can lead to a change of a few orders of magnitude in conduction of the junction [23, 48, 49]. In the case of alkane(di)thiol molecules this difference in conduction between physisorbed and chemisorbed contacts can be understood by describing current through the molecular junction with the Landauer formula [10, 25, 49–53], stating that the conductance G is given by:

$$G = \frac{2e^2}{h} \times T_l \times T_{mol} \times T_r,$$

where e is the elementary charge, h Planck's constant and T_l, T_r and T_{mol} are the transmission coefficients of the left contact, right contact and the molecule, respectively. It is clear from this formula that a change in transmission of one of the contacts will change the absolute value of the current with the same factor. Therefore, to make a good comparison between the obtained currents per molecule, the differences in transmission of the second contact must be accounted for. One prime example is the contact difference between alkanemonothiols and alkanedithiols.

3. Molecular electronics testbeds

3.1. Scanning tunneling microscope

A scanning tunneling microscope (STM) scans over a surface with an, preferably, atomically sharp conducting probe. A bias is applied between the STM tip and the conducting substrate and the tunneling current between both is monitored [54]. When the tunneling current is kept constant (constant current mode), the height profile of the surface is recorded. When the position of the probe is kept constant (constant height mode), the change in current is recorded. Often an STM operates best when a combination of both is used, i.e., height and current vary both while scanning the surface. By using a conducting sample, a SAM of alkane(di)thiols on top of a metal film can be studied, see figure 3. Its usability makes STM one of the most widely used techniques to study molecular monolayers [23, 24, 55–63], even though alkanedithiols might chemisorb to the STM tip.
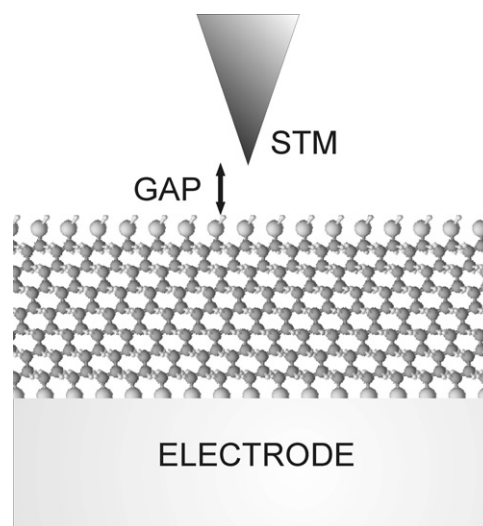
Figure 3. Schematic representation of an STM. The tunneling current between the STM tip and bottom electrode is recorded to measure the conducting properties.

The STM is capable of recording very small currents. This is also a necessity because of the presence of a tunneling gap between the STM tip and the surface studied, that severely lowers the total current between both electrodes. The major advantage of an STM is to record simultaneously the current and morphology of the sample at the atomic level and, therefore, the tip can be used to address and measure at specific locations or molecules. This also implies that single molecules can be measured, but in densely packed SAMs it is never exactly clear how many molecules will be measured since the exact size and morphology of the tip is unknown. To circumvent this problem, conducting molecules embedded in an insulating SAM matrix have been studied [64, 65]. However, this creates other challenges like circumventing the inherent instability of the probed molecules due to the fact that the inserted molecules pack at less dense areas in the SAM, originating from defect sites on the substrate surface and grain boundaries [66]. The major disadvantage of STM arises from its major advantage. Since the STM operates in constant current mode, constant height mode or a combination of both, it is actually unclear what the distance is between the tip and the surface and whether changes in current are due to changes in height or due to a change in conduction of the molecules. Furthermore, because of the additional tunneling distance due to the gap between the molecules and the tip together with the extremely small device areas, lower currents are measured. This is a limiting factor for the maximum measurable length of the insulating alkane(di)thiols, i.e., when the alkanethiols exceed more than ∼14 carbon atoms in length, electrical measurements by scanning tunneling microscopy are extremely difficult [67, 68]. The advantages of using STM are the possibility for studying *in situ* the assembly and performing measurements in solution [62, 69]. This gives rise to the opportunity to measure molecules bridging the gap with both endgroups anchored to the tip and substrate [23, 28–30, 63]. The chemisorbed contact at both

ends greatly reduces the influence of contact resistance on the total resistance. Furthermore, since the tip can be moved repeatedly up and down to fabricate each time a new single molecule junction, statistics can be done and fluctuations due to different contacts will be excluded from the results. Research to develop the STM is still in progress and resulted in video rate STM with frame rates up to 200 images per second while maintaining atomic resolution [70].

3.2. Conducting probe atomic force microscope

Although STM and AFM [71] are often enveloped by the more general term *scanning probe microscopy* [8, 11, 12], significant differences between both techniques lead us to treat them separately in this review. In a conducting probe atomic force microscope (CP-AFM) a conducting probe is brought into contact with the molecules on a conducting substrate (or electrode), see figure 4. By applying a DC bias between the probe and the substrate, electron transport through an ensemble of molecules in the SAM can be studied [72]. In general, the main difference between AFM and STM is the fact that an AFM does not require a conducting substrate. With an AFM the force and deflection of a tip is registered, instead of measuring the tunneling current between tip and substrate. Therefore, AFM is a widely used tool for studying, for example, the morphology of thin polymer layers and polymer structures [73–76]. However, to study the electronic transport though a monolayer of molecules, a conducting substrate acting as electrode is a necessity. The main argument for using an AFM instead of an STM in molecular electronics is the fact that the AFM probe is brought into contact with molecules. This eliminates the current reduction caused by the extra tunneling gap in the STM set-up [77–80]. However, the conducting probe tip of the CP-AFM is coated with a metallic layer, which implies that this tip is also significantly larger than an STM tip and, most likely, not atomically sharp [72, 78]. This induces a higher uncertainty in the number of molecules measured. Furthermore, one has to take the roughness and morphology of the bottom contact into account to make an estimation of the number of molecules under study. Since an STM tip can be localized at a certain position on the nm scale, measurements at every preferred location can be performed with an STM. In the AFM set-up the surface roughness is unimportant when a larger AFM tip contacts atomically flat regions of a surface, such as obtained by annealing Au(111) on mica. With higher surface roughness, however, the amount of molecules making contact to the tip might vary between different measurement sites at the same sample, causing a variation in the obtained current–voltage (*I*–*V*) characteristics [19, 81]. Another application of the AFM is, first, the deposition of a metal nanoparticle on the SAM and, second, contact of the nanoparticle with the AFM tip (NP-AFM) [25, 82, 83]. Since the size of nanoparticles is well defined, the number of molecules contacted is known. Side effects in a metal/SAM/nanoparticle/conducting AFM probe configuration, such as charging of nanometer-sized nanoparticles [83] and the contact resistance between the AFM tip and the nanoparticle do need to be accounted for. With
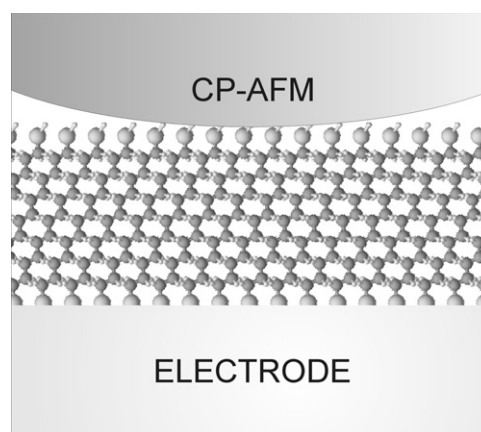

Figure 4. Conducting probe AFM. Schematic representation of a CP-AFM tip in contact with molecules on a conducting substrate. By applying a voltage between the tip and the bottom electrode, electronic transport through a SAM can be studied.

the sensitive AFM cantilever, the applied force of the AFM tip to the substrate can be varied [84, 85] but it remains unclear whether the contact force of the tip to a SAM causes any local deformations or rearrangements of the molecules [26, 72, 84]. Another important aspect of AFM compared to STM, is the possibility to study the effect of chemisorbed and physisorbed contacts. For example, a gold-coated AFM tip brought into contact with an alkanedithiol monolayer might result in higher currents compared to measurements on alkanemonothiols due to the chemisorbed nature of the S–Au bond [20, 48, 49]. Furthermore, since an AFM tip can be coated with different metals, it offers the possibility to determine the influence of metal work function on the electronic transport through the junction. This is a more reliable method than varying the metal of the bottom electrode, since these might influence other features of the SAM, such as packing density and tilt angle [7, 16].

3.3. Break junction

Break junctions can be divided in two classes, mechanically controllable break junctions and electromigration break junctions. The mechanically controllable break junction (MCBJ) was first developed in 1992 [86], based on an earlier design by Moreland and Ekin who studied the tunneling characteristics for super conductors [87]. The technique consists of a lithographically defined metallic free suspended bridge or a notched wire above a gap etched in an insulating (polymer or oxide) layer on a, preferably, bendable substrate (figure 5). A piezo controlled pushing rod bends the substrate with micrometer precision in *z*-direction, while the counter supports at the sides of the sample keep the sample at a fixed position. Bending the substrate leads to an elongation in the plane of the electrodes causing the metallic bridge to break. Due to the high reduction factor between the piezo micrometer precision in *z*-direction and the in-plane elongation, the gap between the electrodes can be altered with sub-nm control [88–92]. This ensures a well-defined distance between the electrodes and a stable configuration of the junction, down
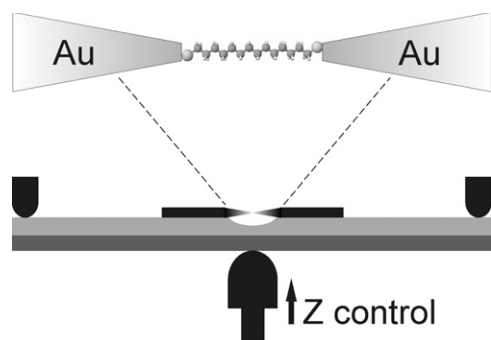
Figure 5. Schematic depiction of a mechanical break junction set-up. A piezo controlled pushing rod bends the substrate with μm control. The large reduction factor between the Z-movement and the elongation in-plane allows for sub-nm control of the electrode distance.

Figure 6. Nanotransfer printing of metallic electrodes onto a SAM. Due to the chemical interaction between the evaporated metallic layers on the PDMS stamp and the end group of the SAM (e.g., S–Au bond), the metallic electrodes will be transferred from the stamp onto the SAM.

to 0.2 pm h^{-1} [88]. The stability is further enhanced by performing measurements at low temperatures [92, 93]. The bendable substrate is most often made from a phosphor–bronze sheet for its superior mechanical deformation properties and an insulating layer of polyimide is spin coated to insulate the contacts from the substrate and to level the surface of the substrate. Polyimide can than be etched underneath the metallic bridge with an rf plasma to make the bridge suspended above the substrate [88, 91, 94–96]. In the final step the molecules can be assembled between the leads. This can be done by different methods; breaking the electrodes while molecules are present either in solution [91] or in the gas phase [96], or by adding a solution with the self-assembling molecules after the contacts are broken [94, 95]. The main advantage of the MCBJ technique is the sub-nm control of the contacts with the possibility to measure single molecules. Furthermore, the back and forth bending of the substrates allows for doing statistics on a large number of measurements with a single junction [27, 96–98]. This is an essential aspect for reliable measurements on single molecules.

Since the local configuration of the electrodes cannot be controlled, the exact configuration of the junction is unknown. From theoretical studies it is clear that the exact shape, configuration and mechanical stress of the electrodes are very important and influencing the outcome of experiments on single atom chains or single molecules [18, 20, 21, 99, 100]. Next to morphology issues related to the use of different metals, as discussed in section 2.1, the conduction from monatomic wires changes for different metals [88, 92, 97, 99], these changes have to be accounted for.

In a break junction formed by electromigration, the gap between two electrodes is created by passing a large electrical current through a lithographically defined nanowire [101, 102]. Due to the high current, electromigration of the Au atoms takes place, resulting in breaking of the nanowire. With this technique a reproducible gap between the two electrodes of typically 1–2 nm is created [32, 101, 103, 104]. This process can be done on rigid substrates such as Si/SiO$_2$ wafers. Since processing equipment is often intended for using standard Si wafers with a certain dimension, fabrication of the electromigration break junctions is complementary with
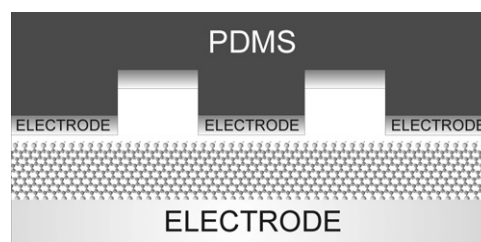
current industrial techniques. However, using a rigid substrate implies that the gap between the electrodes cannot be varied after its formation. When junctions are fabricated with the same distance between the electrodes but with a variation in the length of the molecules, this will result in a different type of junction, mainly at the molecule/electrode interface. Contrary to mechanically controllable break junctions, junctions formed by electromigration cannot perform a large repetitive collection of measurements with the same junction. Therefore, a large number of devices need to be fabricated to do statistics [101]. Furthermore, due to a rigid configuration of the electrodes, the number of molecules in the junction is not accurately known. The size of the electrodes is sufficient for catching tens of molecules when a droplet of the self-assembling molecules in solution is deposited onto the nanogap. The advantages and disadvantages of this technique are similar to those of MCB junctions, except for the lack of control of the gap size between the electrodes. The morphology of the electrodes at the gap has been studied with scanning electron microscopy [105, 106] and *in situ* imaging of the nanogap formation has been done with transmission electron microscopy [107]. From the electron microscopy studies it is clear that the shape of the electrodes is highly irregular. The breaking of the narrow Au finger can result in an asymmetric shape of the junction when breaking occurs while a bias is applied and a symmetric configuration when a final narrow region breaks spontaneously [107]. It is unclear whether this difference in symmetry of the electrodes will lead to a difference in the obtained current per molecule when molecules are inserted in the junction. Furthermore, local heating of the junction during gap formation can increase the temperature up to the melting point of gold, resulting in large gaps and the possibility of gold islands inside the gap [108].

3.4. Nanotransfer printing

Nanotransfer printing (nTP) is a technology where a thin metal layer is transferred from elastomeric stamps as well as hard stamps onto a designated surface [109], for example onto a self-assembled monolayer, see figure 6. Nanotransfer printing is similar to the widely used microcontact printing technique, where surfaces can be patterned by transferring SAMs from a PDMS stamp onto a substrate [110–114]. However, nTP is a purely additive printing technique based on the surface chemistry of the appointed surface, which bonds chemically

with the metallic layer at the stamp. By bringing the stamp with the thin evaporated metallic layer in contact with the substrate, the metallic layer is chemically bonded to the substrate and released from the stamp, resulting in highly reproducible and well-defined structures with nanometer resolution over large areas [115–117]. The most common material used for the elastomeric stamps is poly(dimethylsiloxane) (PDMS). PDMS is patterned by casting and curing a pre-polymer of PDMS on a pattern in a resist layer on a silicon wafer. The resulting pattern in the PDMS stamp is then the negative image of the pattern in the resist layer. Afterwards, a thin metallic layer is evaporated onto the PDMS stamp. Rigid stamps are made from GaAs by locally etching the GaAs with a patterned resist layer as an etching mask.

Since the electrodes or metallic films on the stamp are transferred in their entirety, the resulting structures do not suffer from short circuit formation, as with direct evaporation of metals on SAMs [33–35]. Moreover, due to the chemical interaction between the end group of the SAM and the metallic film on the stamp, a necessity for transferring the electrodes onto the SAM, a chemisorbed contact at both ends of the molecules is ensured. This results in a lower contact resistance, compared to a physisorbed contact [23, 48, 49]. It also implies that the difference between chemisorbed and physisorbed cannot be investigated with this method. The bottom electrode roughness is of less importance for the elastomeric PDMS stamps compared to the rigid GaAs stamps, since the flexible PDMS will adapt to small variations in height. Due to the ∼100 nm scale of the top contacts, differences in height will be limited to a minimum and roughness of the bottom contact might be a non-critical factor. More important is the size and aspect ratio of the pattern on the stamp in order to determine the number of molecules under study. It was found that the edge resolution can be as high as 5–15 nm, comparable to the grain size of the Au. Furthermore, a rigid stamp will not deform when it is brought in contact with a substrate, but elastomeric stamps are easily deformed when a small force is exerted on the stamp, which has to be accounted for when the final device size is determined. Any possible local deformations or reorganization of the SAM when a stamp is brought in contact with the molecules might be influencing the outcome of the measurement; hence this technique ideally allows for a simultaneous fabrication of many different electrode patterns and sizes to perform profitable statistics on the data obtained [117].
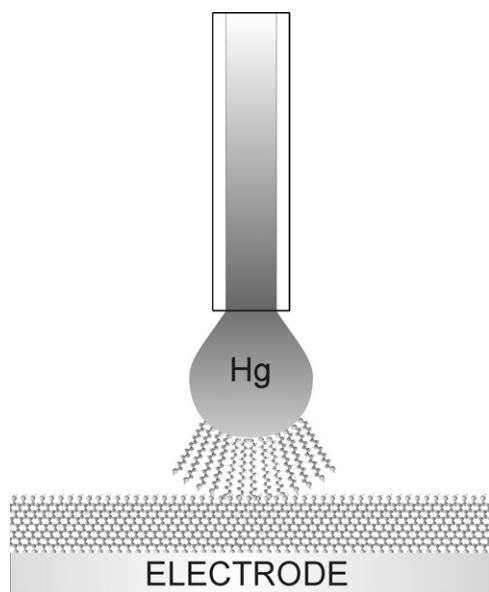
3.5. Hanging mercury drop junction

As described in the section 1, first experiments to measure the electronic properties on molecular monolayers used mercury as a top electrode onto a SAM [4]. The first well-defined hanging mercury drop electrodes (HMDE), coated with a molecular monolayer were fabricated to mimic a biological membrane [118]. By a clever combination of both concepts, a molecular junction of Hg–SAM–SAM–metal with a well-defined area [119–121] can be fabricated, see figure 7. When the second metal electrode is also Hg, the processing is relatively straightforward and leads to very reproducible

junctions. In a glass capillary two drops of Hg are brought in contact. The area is defined by the cross section of the capillary and the distance between the Hg drops by the length of both SAMs. Since alkanethiols have a very high affinity for Hg and form a densely packed SAM on the defect free surface of the Hg drop, the junctions are well defined [119, 121]. Moreover, since alkanethiols are perfectly perpendicular oriented with respect to the Hg surface, the exact configuration of these tunnel junctions is known [7, 120, 122–124]. When the second electrode is not Hg but a metallic layer, junctions can be made repeatedly with the same mercury drop at the same location of the bottom contact substrate. Moreover, the simplicity of this technology allows for performing measurements on a large number of molecular junctions at different sites on one substrate, but also for measuring on different substrates. Therefore, large amounts of data can be collected rapidly for different situations. This will ensure the validity of statistics on the data and results in reproducible molecular junctions. When a bottom electrode on a substrate is used, other aspects also play a role for the junction quality. Firstly, the bottom contact roughness is a critical factor. Abrupt changes in height will not be compensated for by the Hg drop and the solvent for the SAM might remain partially in the junction or the contact area might be locally distorted [19, 121]. Secondly, the device area can be varied but the area has to be determined with high accuracy to calculate the current density or the current per molecule [125–127]. Thirdly, different bottom electrode metals will result in a change in tilt angle of the first SAM and this gives rise to a less defined contact between both SAMs and this has to be taken into account together with the change in work function [7, 121, 128–130]. Finally, Hg has a high affinity for Au and they form an amalgam easily. The adsorption of Hg by Au films is an irreversible process which leads possibly to short circuit formation in hanging Hg drop experiments when defects are present in the SAM [131–134]. By using a bi-layer of SAM the possibility for short circuit formation is greatly reduced and the reproducibility is increased [120, 121, 135]. This is also a limiting factor since the study of a single SAM (e.g., the current dependence on the length of alkanethiol SAMs) can only be performed by comparing relative changes when one SAM is altered with respect to the total junction.

3.6. Nanopores

Direct evaporation of metals on top of SAMs is likely to result in filamentary growth of metals through the SAM and thus short circuits are created [33–35]. The number of metallic pathways through the SAM is mainly dependent on the number of defect sites in the SAM, which increases with device area. When extremely small device areas are fabricated with a device area smaller than the domain size of the SAM, the SAM might be defect free and metal contacts can be created via vapor deposition [136]. Evaporation with a low evaporation rate further reduces the possibility for metal atoms to penetrate the SAM [136, 137]. Another improvement might be cooling of the substrate during evaporation [137], but it is under debate if this indeed improves the yield of working devices [138, 139]. The creation of a nanopore

Figure 7. Schematic representation of a hanging mercury drop experiment. The Hg–SAM–SAM–metal junction is fabricated by coating a controlled drop of Hg with a SAM and bringing this drop with SAM in contact with a metal surface containing another SAM. By applying a bias voltage over the Hg and metal bottom electrode the electrical properties of a double layer of SAM can be measured.
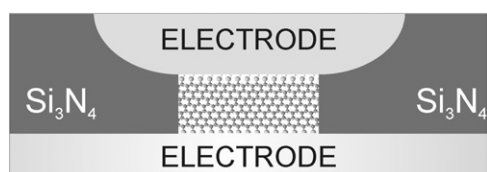
Figure 8. Schematic representation of a nanopore device. The device diameter is typically in the range of 30–60 nm, i.e., smaller than the domain size of the SAM. The nanopore is fabricated in a Si_3N_4 membrane by E-beam lithography and plasma etching. A densely packed SAM of a single domain can prevent the penetration of metal atoms through the SAM when a metal contact is evaporated.

or nanowell is done in an insulating material like SiO_2 or Si_3N_4 [136, 139, 140]. The insulation layer can be etched away locally using E-beam lithography and plasma etching or focused ion beam, resulting in nanopores with a typical diameter between 30 and 60 nm. By inspection with a SEM, the device area can be verified to nm accuracy [141, 142]. The substrate underneath the etched layer can be any metal or semiconductor suitable for SAM formation [7, 138, 143]. In the final step the top contact is evaporated on the other side of the substrate on top of the SAM, see figure 8.

This technology offers a number of significant advantages compared to many other molecular junction testbeds. A large number of devices can be made simultaneously, i.e., large arrays of nanopores can be fabricated by E-beam lithography. This allows for determining the device yield out of a large collection of devices and statistics can be done on the data obtained for the working devices [136, 138, 139]. Since the device area can be controlled and measured accurately, the number of molecules in the junction is known with high
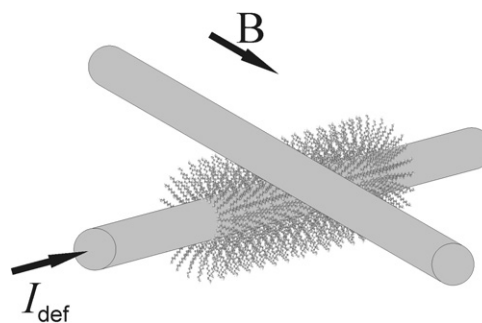
Figure 9. Schematic representation of a crossed wire junction with one wire coated with a SAM perpendicular to the applied magnetic field B. The low current through the wire coated with a SAM creates a Lorentz force, by which both wires can be brought into contact and the electrical transport through the SAM can be studied.

accuracy. Furthermore, the metal is evaporated directly onto the SAM, creating an intimate contact between the metallic electrodes and the molecules, independent of the end group of the SAM. The fact that the working devices are not shorted does not provide a guarantee for a perfect layer of metal on top of the SAM. Perhaps a partial penetration of Au atoms takes place into the SAM. A clear indication for this fact is provided by the yield of working devices when only the type of SAM and the bottom electrode material are changed in the same junction configuration, fabricated by the same method. By changing the backbone of the SAM and the type of substrate, the packing density of the molecules in the SAM will be different [7, 16]. With a larger spacing between the molecules the probability of metal filament formation in the SAM will increase. The yield for the same type of nanopore junctions can decrease from 80% working devices to as low as 6% when only the type of SAM and bottom electrode are changed [136, 138]. Another major advantage for the use of nanopores is the possibility to do temperature dependent measurements. These are crucial for determining the direct tunneling mechanism for conduction through alkane(di)thiol monolayers [11, 141]. The nanopore junctions are stable and can be measured in any measurement station and temperature dependent measurements can be performed. Although reasonable variations in device area can be easily made with this technology, the area of the nanopores has an upper limit defined by short circuit formation and a lower limit by pore opening or E-beam resolution. Both limits are within the same order of magnitude (30–60 nm), therefore, large changes in device area cannot be achieved.

3.7. Crossed wires

A recent method for the fabrication of a molecular junction is the so-called crossed wire junction [144]. The concept of the crossed wire junction is schematically illustrated in figure 9.

To fabricate a crossed wire junction, two metallic wires of 10 μm in diameter are mounted on a test stage in a crossed geometry. One of the wires is covered with a SAM and perpendicular to an applied magnetic field (B). A small current (I_{def}) through this wire controls the deflection of this wire by the generated Lorentz force. Therefore, the two

wires can be brought into contact gently and the electrical transport characteristics can be measured by applying a voltage between both wires [145, 146]. Since different metallic wires can be used [147], the change of work function and junction asymmetry can be studied. Moreover, due to the perfect control of the deflection of one of the wires, the contact force between the wires can be varied by small amounts. Therefore, it is possible to do experiments on scaling of molecular junctions, i.e., more molecules are contacted when the deflection current in the wire is increased [148, 149]. These changes in contact can be as large as contacting between 1 and ~1100 molecules by increasing the deflection current [148]. The number of molecules in the junction was determined afterwards by dividing the obtained I–V characteristics by integers. The exact amount of contacted molecules by both wires during a measurement is unfortunately unknown. Furthermore, how a SAM is exactly oriented on a curved surface is unclear, but the relatively large diameter (10 μm) of the wire eliminates most likely this issue. With the relatively large radius, the local surface curvature of the wire at the place of contact (for a maximum ~1000 molecules) is minimal. The small local surface curvature of the wire might even be the reason why the contact area between different experiments can be varied with such accuracy.

3.8. 2D nanoparticle array

A recent method for measuring in-plane the transport through a large collection of molecular junctions involves the formation of a Langmuir–Blodgett monolayer of nanoparticles on a large scale. The Langmuir–Blodgett monolayer consists of gold colloidal nanoparticles encapsulated with alkanethiols [150]. To fabricate the large scale array, gold particles of a few nm in diameter can be encapsulated with alkanethiols by mixing a gold nanoparticle ethanol solution with an alkanethiol solution [151, 152]. After separation of the encapsulated gold nanoparticles from the ethanol, the nanoparticles can be dispersed in chloroform. The dispersed suspension of the alkanethiol-encapsulated gold nanoparticles in chloroform can be cast by the Langmuir–Blodgett technique to get a monolayer of nanoparticles over an area of several micrometers squared [153]. Best results with this method were obtained by using an alkanethiol concentration above 0.1 mM and a gold nanoparticle concentration between 0.06 and 0.3 mg ml^{-1}. With these conditions the monolayers are formed with a hexagonal packing of the encapsulated nanoparticles and exhibit long range order [151, 153]. Moreover, when the monolayers are formed on a water surface the long range uniformity can be increased to macroscopic scales [154]. These uniform monolayers of several millimeters squared on a water droplet can be transferred by microcontact printing with a PDMS stamp to different substrates, preserving the uniformity of the monolayer [150, 154]. By structuring the PDMS stamp with parallel lines and evaporating top contacts, a well-defined two-dimensional array of alkanethiol-encapsulated gold nanoparticles can be fabricated [150]. The resulting structure of the array is schematically depicted in figure 10. Since the monolayer is extremely uniform between
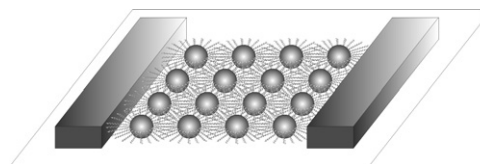

Figure 10. Schematic representation of a 2D nanoparticle array measurement. Gold colloidal nanoparticles with a diameter of 10 nm are encapsulated with alkanethiols, after which a two-dimensional array of nanoparticles is transferred by PDMS stamping onto a substrate into parallel lines. By evaporation of two larger electrodes the I–V characteristics of the encapsulated nanoparticle array (~1000 molecular junctions in series) can be measured.

the two electrodes, consisting of ~1000 molecular junctions in series, the resistance of one molecular junction (R_J) can be accurately estimated by measuring the sheet resistance (R_{TOT}) of the monolayer. By modeling this array as a hexagonal network of nodes interconnected by identical molecular junctions the resistance of one molecular junction will be given by $R_J = (2/\sqrt{3}) \times R_{TOT}$ [150]. By measuring with this clever method many junctions at once, a reproducible average of different molecular conformations is obtained. Stability of the junctions is ensured by the well-defined structure of the array. Although the gold nanoparticles in these networks are only 10 nm in diameter, it is unclear by how many molecules two neighboring nanoparticles are contacted. Furthermore, the junction resistance deduced from the sheet resistance will decrease slightly when gold nanoparticles will contact each other or increase when defect sites are present in the array. By electron microscopy it was found that virtually all particles are separated with equal spacing and number of defect sites is very low compared to the number of nanoparticles [150, 154], resulting in an accurate estimation of the junction resistance.

3.9. Large area molecular junction

A very recent technology for the fabrication of molecular junctions with large devices areas, incorporates a conducting polymer as a top electrode [11]. The devices are fabricated in an insulating photoresist matrix for exact control of device area and to prevent degradation of the device in ambient conditions. Au bottom contacts are first evaporated on a Si/SiO$_2$ wafer and photoresist is spin coated. By standard photolithography vertical interconnects are made in the photoresist layer ranging from 10 to 100 μm in diameter. After the self-assembly of the monolayer in the vertical interconnects on the bottom electrode, a water-based suspension of poly(3,4-ethylenedioxythiophene) stabilized with ploy(4-styrenesulfonic acid) (PEDOT:PSS) is spin coated over the wafer. PEDOT:PSS is a commercially available highly conducting polymer and comes in a wide range of conductivities and viscosities. The final step in the processing is the evaporation of a gold top contact on top of the PEDOT:PSS, which not only ensures a good contact of the measurement probes to the device, but also acts as an etching mask when the redundant PEDOT:PSS is etched away using reactive ion etching to prevent parasitic currents form top to bottom electrode when probed [11, 31]. The cross
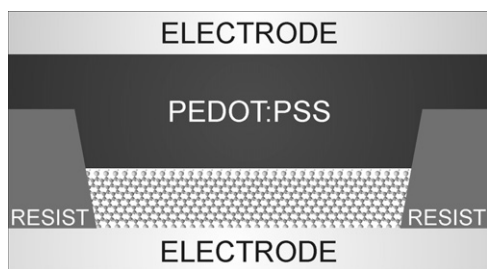
Figure 11. Schematic cross section of a large area molecular junction. The devices are processed in an insulating photoresist matrix to protect de device from degradation in ambient conditions and to allow for an easy variation of device area. A top contact of the highly conducting PEDOT:PSS is spin coated on top of the SAM. The molecules of PEDOT:PSS are too large and too hydrophilic to penetrate the SAM and short circuit formation is therefore prevented.

Figure 12. A nanoparticle bridging the gap between two electrodes covered with a SAM, forming a double molecular junction in series. After the creation of the two electrodes separated by a small gap, a SAM is applied to the electrodes and a nanoparticle is trapped in the gap by an alternating electric field or by a magnetic field.

section of a large area molecular junction is schematically depicted in figure 11. The macromolecules of the PEDOT:PSS are too large to penetrate the densely packed SAM and PEDOT:PSS is too hydrophilic to penetrate the hydrophobic interior of the SAM. Consequently, the formation of short circuits is prevented. As described in section 3.6, the direct evaporation of metals on SAMs for extremely small devices is possible when the domain size of the SAM is larger than the device area [136]. However, when device areas are larger, the evaporation of metal electrodes results in short circuit formation and a typical yield of ∼1% of working devices is obtained [33, 36].

The use of a conducting polymer as a top electrode on top of a SAM in an insulating photoresist matrix has proven to result in a device with a stability of at least several months in air, no degradation upon sweeping, and working devices with diameters up to 100 μm. Furthermore, the yield of working devices is close to 100% and the technology is compatible with standard integrated circuit fabrication processes [11]. Large area molecular junctions have a number of advantages in common with the nanopores. Temperature dependent measurements are easily performed, a large collection of devices is fabricated simultaneously and the device area is well defined. Besides these similarities, a number of significant differences are present. The device area of nanopores is limited to a maximum of 60 nm in diameter, whereas the large area molecular junctions have a device area range of several orders of magnitude, i.e., device range from 10 to 100 μm in diameter. This also implies that measurements in large area molecular junctions are not done on a monodomain of a SAM, as was done in the nanopores. The SAM in a large area molecular junction will be less ordered and can contain pinholes. This has to be accounted for when the current per molecule is calculated. Furthermore, in the nanopores experiment, the intimate contact between the electrodes and the molecules is better defined than the contact of PEDOT:PSS to the molecules. The exact nature of this PEDOT:PSS/molecule physisorbed contact is not yet established. In a spin coated PEDOT:PSS film lamellas of PSS separate pancake-shaped PEDOT-rich islands [155]. Therefore, it is unclear whether the
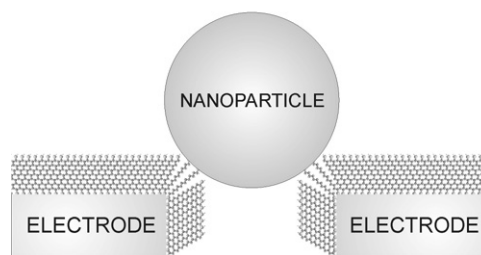
molecules are contacted at the molecule/PEDOT:PSS interface by the more conductive PEDOT regions, by the PSS, or both. A strong indication for the latter is provided by the perfect overlap in current density for a device ranging from 10 to 100 μm in diameter. Furthermore, the analysis of the PEDOT:PSS morphology, albeit for a different type than used for the large area molecular junctions, shows that the PEDOT-rich islands are typically 20–25 nm in length and 5–6 nm in height [155]. Furthermore, since the PEDOT:PPS is a water-based suspension, spin coating on a SAM with a hydrophobic end group will be difficult and results possibly in pinholes in the PEDOT:PSS layer. As with all measurements on devices containing a large number of molecules, differences in local molecular confirmation, binding sites and contacts will be averaged, resulting in reproducible measurements.

Another technique to fabricate large area molecular junctions combines the hanging mercury drop technique with the previously described fabrication of large area molecular junctions. By spin coating a thin film of the semiconductor poly[(*m*-phenylenevinylene)-*co*-(dioctoxy-*p*-phenylenevinylene)] (PmPV) on top of a SAM, the formation of short circuits is prevented. The contact to PmPV is made by a hanging mercury drop as described in section 3.5 [156]. With this method the use of a bi-layer of SAM is no longer a requirement and single monolayers of SAMs can be investigated.

3.10. Nanoparticle bridge molecular junction

A nanoparticle bridge junction (NP bridge) is a hybrid assembly technique to fabricate a molecular junction. Two electrodes separated by a small gap are fabricated by *E*-beam lithography [157], electromigration [158] or oblique angle evaporation [159]. A monolayer is self-assembled on to the electrodes and nanoparticles are deposited to bridge the gap (figure 12).

There are several methods to trap gold nanoparticles within the gap. The first reported method is by trapping deposited nanoparticles in the gap by applying an alternating electric field [157]. Commercially available Au colloids in water can be suspended on the substrate and an ac bias is applied to the electrodes. The nanoparticles are pulled in the direction of the maximum field strength, i.e., within the

gap. Another method is by trapping Au-coated magnetically susceptible silica colloids in a local magnetic field between the electrodes, containing a ferromagnetic core [160, 161]. By applying an external magnetic field, the ferromagnetic core of each device is aligned and the magnetically susceptible nanoparticles are trapped at the maximum magnetic field within the gap. Other methods for trapping nanoparticles require simply evaporating gold at the gap region at slow evaporation rates [158] or the deposition of Au nanoparticles from solution on the electrodes [159]. The latter methods are less controlled than trapping nanoparticles of specific size at a well-defined location. The deposition of the nanoparticles to bridge a gap between electrodes is a relatively simple and reproducible processing technique where the diameter of the nanoparticles is related to the distance between both electrodes. An increase in gap size between electrodes implies an increase in nanoparticle size and thus a variation in the number of molecules under study. Furthermore, the technology offers new possibilities when the gap and nanoparticles are sufficiently small for the metal nanoparticles to be charged noticeably by single electrons [158]. The number of molecules contacted by the nanoparticle at each electrode is unknown, but relative changes in current are easily observed when different types of molecules are inserted. Since the nanoparticles bridging the gap cannot be contacted by macroscopic probes, two molecular junctions in series, a double junction, is the result. This gives rise to an uncertainty when the absolute value of the current per molecule at a certain bias needs to be determined. However, with sufficiently large nanoparticles where charging effects can be neglected and the nanoparticle can be regarded as a bulky contact, this problem is avoided since the voltage drop over both junctions will be equal for an applied bias over the electrodes.

3.11. Soft contact deposition

Soft contact deposition techniques for applying a top electrode to a molecular monolayer, without the formation of short circuits or damaging the monolayer, can be divided in the lift-off–float-on (LOFO) process and the polymer-assisted lift-off (PALO) process. In the LOFO process, a thin metal film is detached from a suitable solid support in a specific solvent [162]. The detachment of the metal film from the substrate can be done when the binding to the substrate is weak. When the binding is strong, such as Al/SiO$_2$, a sacrificial layer can be used between the substrate and metal film that can be etched away selectively [162]. Dipping the substrate in a suitable solvent at the moment when the metal film starts to detach, will results in the floating of the metal film on the liquid. The metal film can than be transferred to another substrate with pre-patterned metal electrodes with a SAM. The repulsion between the floating metal film and the substrate is lowest when one of them is hydrophobic [162]. The amount of wrinkling and tearing of the metal film on the substrate is reduced by a rapid evaporation of the solvent. The PALO process combines the soft contact deposition advantages of LOFO with the advantages of patterning freedom of nanotransfer printing [163]. The main difference between
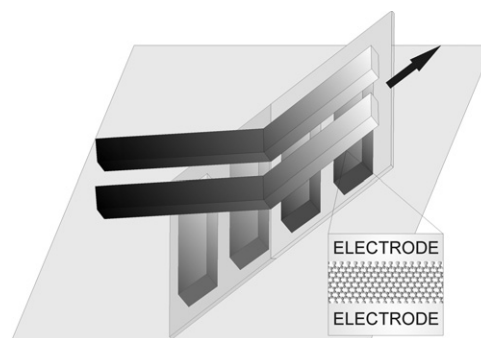
Figure 13. A schematic depiction of the final stage of the PALO process. Multiple floating electrodes stabilized by a polymer layer can be transferred from a liquid surface onto a substrate with pre-patterned electrodes covered by a SAM to form a large number of molecular junctions at once. The technique allows for a wide range in device areas and the obtained yield of non-shorted devices is >90%.

PALO and LOFO is the use of a polymer layer on top of a sacrificial substrate with patterned metal electrodes. The polymer layer is then detached together with the electrodes from the substrate onto a suitable liquid surface. The polymer layer allows for the transfer of many electrodes simultaneously and ensures stability of the electrodes by preventing wrinkling and tearing of the metal films. The collection of electrodes can then be transferred onto a substrate with multiple metal electrodes covered with a SAM (figure 13). Many junctions can be fabricated simultaneously and device areas range from 100 μm^2 to 9 mm^2 [163]. Furthermore, the deposition of metal electrodes with this soft deposition technique results in a yield of greater than 90% non-shorted devices. This high yield of working devices together with the possibility to fabricate a large number of molecular junctions in parallel allows for doing excellent statistics on the obtained data.

The presence of solvent between the SAM and the top electrode must be avoided. An intimate contact between the metal film and the molecules will be the most likely result due to capillary forces when a suitable solvent is used [162]. The soft deposition method combines a number of advantages from different techniques, i.e., an intimate metal/molecule top contact, assemblies of molecules can be measured, a reproducible averaged electrical transport characteristic, and statistics are easily obtained due to the possibility of processing multiple junctions at once with a high yield of working devices.

3.12. Metal evaporated molecular junction

As discussed in previous paragraphs, the direct thermal evaporation of metals on a molecular monolayer is likely to result in filamentary pathways of metal atoms through the monolayer, specially at pinhole defect sites in the SAM [33–35]. The possibility of metal penetration is greatly reduced by decreasing the device area to a dimension smaller than the domain size of the SAM, as was done in the nanopores experiment [136]. For larger device areas, the short circuit formation can be reduced by using the so-called cold-gold evaporation technique [164]. With cold-gold evaporation, macroscopic contacts can be evaporated onto glass substrates
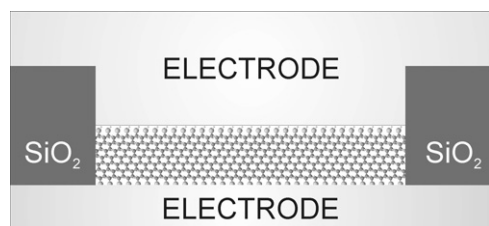
Figure 14. Schematic cross section of a molecular junction fabricated in a vertical interconnect through an insulating oxide layer, with the top electrode thermally evaporated. Although the yield of working devices is extremely low, by making a huge collection of devices a substantial amount of working devices can be obtained.

Figure 15. Resistance per molecule obtained in different experimental testbeds (references are given between brackets) versus the number of carbon atoms in the alkane chain. By varying the length of the molecules the decay factor β_N can be determined.

containing patterned electrodes covered with a monolayer. The sample is loaded in the vacuum chamber of the evaporator facing away from the boat. The samples are mounted on a copper block cooled by liquid nitrogen. The vacuum chamber is purged with Argon and is kept afterwards at a constant Ar pressure. The evaporated Au atoms from the boat will release most energy in collisions with the Ar atoms, before they land on the cooled substrate. Since the technique relies on scattered Au atoms to land on the side of the substrate facing away from the boat, the deposited thickness was reported to be only 17 nm for every 600 nm recorded by the quartz crystal monitor; the latter is directly in line with the evaporation boat [164]. Another method to fabricate molecular junctions on the micrometer scale with a vapor-deposited top contact, is by simply making a very large amount of devices [36]. Schematically depicted in figure 14, Kim *et al* fabricated 13 440 devices by this method with a diameter of 2 μm. The devices in vertical interconnects were fabricated by reactive ion etching of SiO_2, covering structured electrodes on a Si/SiO_2 wafer. After the formation of the SAM inside the holes, top electrodes were evaporated. 156 working devices were measured by this method, out of the total 13 440 devices fabricated [36]. The yield of working devices is thus ∼1.2%. Clearly, 156 devices are a large collection of working devices to perform statistics on. Therefore, although the technology can be discarded for future applications in industry, valuable experimental data can be obtained by this method. The intimate contact by the metal and the molecule on both sides reduces greatly the influence of the contacts on the current obtained through these junctions. Furthermore, the data obtained from the large number of molecules can easily be compared to experiments with the same device structure, but on a much smaller scale, such as the nanopores. Partial penetration of metal atoms into the monolayer, but not short circuiting the bottom and top contact, cannot be excluded and has to be included in the statistical analysis of the results.

4. Comparison of reported data on currents through alkane-based molecules

To compare reported conduction values on alkane-based single molecules or SAMs, we limited ourselves to published data within the last 5 years (2002–2007). For research groups that published multiple articles on alkane-based molecules with
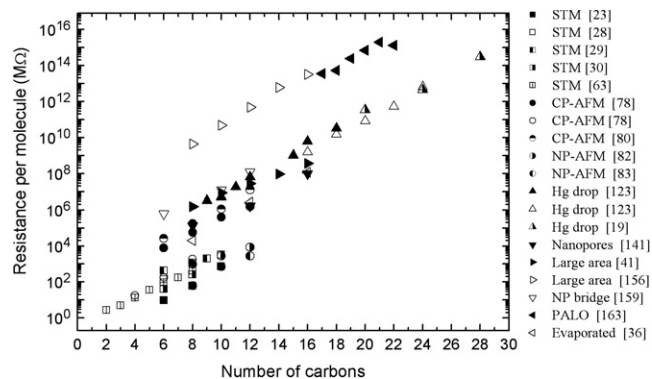
one type of molecular junction, most recent published results were used. Furthermore, instead of concentrating on the true molecule lengths in the junctions, which commonly include bond lengths to the electrodes, we used the number of carbon atoms in the alkane chain. In the case of expressing the length in the number of carbons, unknown bond lengths and undefined contacts are considered to be incorporated in the contact resistance and simply raise the absolute value of the obtained contact resistance. This comparative study is thus primarily focused on the exponential decay of current along the backbone of the alkane chain, excluding the fundamental physics behind the resistance originating from the electrode/molecule interface. However, by comparing the absolute values for the conduction per molecule obtained in different experiments, the relative changes due to different end groups or electrodes can be quantified. Furthermore, certain assumptions were made to calculate the resistance per molecule. Firstly, when the number of molecules in the molecular junction is not specifically mentioned, the grafting density of alkane(di)thiols is assumed to be equal to the maximum grafting density of alkanethiols on Au(111), i.e., 4.6×10^{18} m^{-2} [7]. This applies to reported data where the current or resistance is given per unit area, or when only the device area is mentioned. Secondly, when the device areas of the molecular junctions vary in size and the specific device area used for the reported data is not given, a device area in between the reported minimum and maximum device area is assumed to calculate the number of molecules in the molecular junction.

In general, the current (J) through a molecular tunneling barrier will decrease exponentially with increasing molecule length (d), i.e., $J \propto \exp(-\beta d)$ [11, 28, 79, 82, 141], where β is the decay constant in Å^{-1}. When the resistance per molecule (R_{mol}) is plotted versus number of carbon atoms in the alkane chain (N), the decay constant per carbon (β_N) can be obtained with $R_{mol} = R_0 \exp(\beta_N N)$, where R_0 is the contact resistance [78]. The reported results within the last five years on the length dependence of alkane-based molecules are plotted in figure 15 and listed in table 1, where all data is converted to resistance per molecule using the above-mentioned considerations.

Table 1. Comparison of the measured decay coefficient β_N for alkane-based molecules in different molecular junctions and by different research groups, within the last five years.

| Number of carbons (N)	Contacts	Technique	Number of molecules[a]	β_N (per carbon)[b]	Figure 15	Reference
6, 8, 10	Au–S/S–Au	STM	1	1.09	■	[23]
6, 8	Au–S/S–Au	STM	1	0.99	□	[28]
6, 8, 9	Au–S/S–Au	STM	1	0.51	◧	[29]
6, 8, 10	Au–S/S–Au	STM	1	1.09	◪	[30]
2, 3, 4, 5, 6, 7, 8	Au–NH$_2$/NH$_2$–Au	STM	1	0.86	⊞	[63]
6, 8, 10, 12	Au–S/CH$_3$–Au	CP-AFM	100–1000	0.88	●	[78]
4, 6, 8	Au–S/S–Au	CP-AFM	100–1000	1.16	○	[78]
6, 8, 10, 12	Au–S/CH$_3$–Au	CP-AFM	1000	1.01	◓	[80]
8, 10, 12	Au–S/S–Au	Nanoparticle AFM	1	0.54	◑	[82]
8, 10, 12	Au–S/S–Au	Nanoparticle AFM	1	0.95	◐	[83]
9, 10, 11, 12, 15, 16, 18	Au–S/S–Hg	Hanging Hg drop junction	2.5×10^{11}	1.06	▲	[123]
16, 18, 20, 22, 24	Au–S/S–Hg	Hanging Hg drop junction	2.5×10^{11}	1.01	△	[123]
20, 24, 28	Ag-S/S–Hg	Hanging Hg drop junction	3.7×10^{11}	0.85	▲	[19]
8, 12, 16	Au–S/CH$_3$–Au	Nanopores	7300	0.83	▼	[141]
8, 10, 12, 14, 16	Au–S/SH–PEDOT	Large area junction	3.2×10^8–3.6×10^{10}	0.66	►	[41]
8, 10, 12, 14, 16	Au–S/CH$_3$–PmPV	Large area junction	3.2×10^{11}–3.2×10^{12}	1.13	▷	[156]
6, 10, 12	Au–S/CH$_3$–Au/Au–CH$_3$/S–Au	Nanoparticle bridge	100	0.87	▽	[159]
17, 18, 19, 20, 21, 22	Al$_2$O$_3$–O$^-$CO/CH$_3$–Au	PALO	9.2×10^{12}	0.85	◄	[163]
8, 12, 16	Au–S/CH$_3$–Au	Thermally evaporated	1.5×10^7	1.08	◁	[36]

[a] To calculate the number of molecules in the junctions, the maximum grafting density of 4.6×10^{18} m^{-2} for alkanethiol molecules on Au(111) is assumed.
[b] The decay constant β_N is determined from figure 15.

Figure 15 demonstrates that in all experiments an exponential increase of the resistance with increasing molecule length or the number of carbons in the alkane chain is observed. At first glance, the trend for the resistance increase with an increasing number of carbons in the alkane chain looks similar for each experiment, irrespective of the experimental testbed used. The obtained decay factors (β_N) from figure 15 are listed in table 1.

The calculated values of β_N range from 0.51 to 1.16, with an average value of 0.92 ± 0.19, where the error represents the standard deviation. From the vast majority of these testbeds the same β_N value is calculated within the error. However, some experiments lead to lower [29, 41, 82] or higher [78, 156] values for β_N, outside the range defined by the standard deviation. The reason for a significant different value of β_N that deviates from the value obtained by the majority of the experiments is unclear. No clear correlation is observed between the different values of β_N obtained from similar molecular junctions, and the different experimental conditions of these experiments. For example, two experiments using an STM to contact a single alkanedithiol molecule on both sides, creating a molecular junction between the Au-coated tip and the Au substrate, with 2 chemisorbed contacts, find completely different values for β_N [23, 29]. The data plotted in figure 15 from Xu and Tao leads to $\beta_N = 1.09$ [23] and the data from Haiss *et al* leads to $\beta_N = 0.51$ [29]. Both groups use three alkanedithiol molecules that differ in length to determine the decay factor. The only noticeable difference between the experiments is the number of repeated measurements, where Xu and Tao performed on average ∼20 times more repeated measurements to obtain the average conduction for each molecule and have, therefore, determined β_N, most likely, with higher accuracy. However, a general trend where β_N is related to the number of repeated measurements was not observed, e.g., the data from York *et al* is obtained from only 5–10 measurements per molecule and they calculate a β_N of 1.06 ± 0.04 [123]. Another clear example is the data from the two large area molecular junction experiments. In both cases, a polymer is applied on top of the SAM, before the fabrication of the metal top electrode. The data obtained from the Au/SAM/PEDOT:PSS/Au junctions by Akkerman *et al* results in $\beta_N = 0.66$ and the data from the Au/SAM/PmPV/Hg junctions results in $\beta_N = 1.13$. To further illustrate the spread in the obtained β_N values, β_N versus the number of molecules
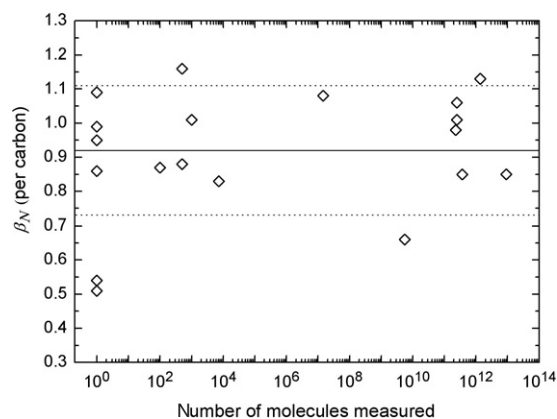
Figure 16. Decay constant β_N versus the number of molecules in the molecular junction. Values of β_N range from 0.51 to 1.16, with an average value of 0.92 ± 0.19. The solid line represents the average value of $\beta_N = 0.92$ and the dotted lines the standard deviation (± 0.19) from this average. The majority of all experiments find a decay constant β_N within this error and the obtained value is independent of the experimental technique used.

Figure 17. The obtained resistances per molecule with increasing length can be categorized into three groups; a low resistance ($\triangle$, $R_{mol} \approx 50$–10^3 MΩ for C8), a medium resistance ($\square$, $R_{mol} \approx 10^4$–10^6 MΩ for C8) and a high resistance group ($\diamondsuit$, $R_{mol} \approx 10^9$–10^{10} MΩ for C8).

in the molecular junctions of different experiments is plotted in figure 16, where the solid line at 0.92 represents the average β_N from all experiments and the dotted lines represent the standard deviation (± 0.19) from this average value. Clearly, the vast majority of all experiments calculate a β_N parameter within the error given by the standard deviation from the average value. Therefore, it can be concluded that, irrespective of the molecular electronics testbed used, similar values of β_N are obtained. Similar plots were made by the authors for β_N versus the number of repeated measurements performed to obtain the average conductance value, and for β_N versus the number of different alkane(di)thiol molecules used to establish β_N. Both plots did not show any obvious trend, demonstrating the validity of the claim that the observed exponential decay factor is independent of the experimental testbed used.

Besides the similar trend in the exponential increase in resistance with increasing molecule length, something more striking can be observed in figure 15. Despite of the different contacts, the molecular end groups, and/or the experimental testbeds that were used, the obtained resistance per molecule as plotted in figure 15 can be categorized in 3 resistance regimes. This is more clearly illustrated in figure 17, where each resistance regime is given a different symbol. The low resistance collection of data (open triangles) is dominated by the single molecule measurements, the medium resistance regime (open squares) encompasses measurements performed on a SAM and the high resistance group (open diamonds) contains the experiments where an extra resistive layer is present in the molecular junction. To illustrate the major differences between these three groups, a linear fit is plotted through all the data from each group. The low resistance group has an average contact resistance (R_0) of 0.8 MΩ and a decay constant (β_N) of 0.76. Both values increase for the medium resistance group to $R_0 = 54$ MΩ and $\beta_N = 1.05$. For the high resistance group R_0 is even 6.1×10^6 MΩ, but $\beta_N = 0.92$, equal to the average value obtained from all experiments (figure 16).
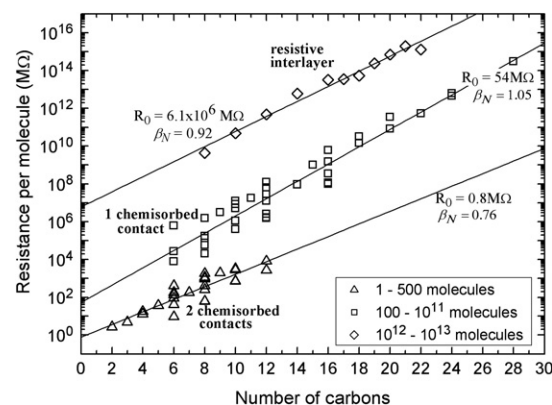
The origin for only three resistance subgroups is related to the nature of the contacts of the molecular junction under study. This is clearly demonstrated by the data from Engelkes *et al*, who performed CP-AFM measurements on alkanemonothiol and alkanedithiol monolayers with a gold-coated AFM tip [78]. The measurements on alkanedithiol monolayers, where both ends of the molecules are chemically bound to the electrodes by the Au–S bond, resulted in a lower contact resistance compared to the measurements on alkanemonothiol monolayers. The measurements with the same experimental set-up on molecules chemically bound at one or at two sides leads thus to a significant difference in resistance. The reported data of Engelkes *et al* on alkanedithiols are within the low resistance group and the data on the alkanemonothiols in the medium resistance group [78]. In fact, all data in the low resistance group is obtained from experiments where molecules are contacted at both ends by a chemisorbed contact.

The difference in resistance by changing the nature of the contacts is clearly illustrated by plotting the resistance per molecule for C8 and C12 versus the number of molecules measured simultaneously in the junction, see figures 18(a) and (b). C8 and C12 are chosen since these are the only molecule lengths represented in all three resistance groups. Furthermore, to make the most reliable comparison, data is added from mechanically controllable break junctions [98] and 2D nanoparticle array experiments [150] to figure 18(a), which were omitted in figures 15 and 16 since no length dependence of the current was investigated. The spread in absolute value for the molecular resistance for both C8 and C12, when the resistance is converted to that of a single molecule, spans at least 8 orders of magnitude. The lowest resistance is obtained for molecules which are chemisorbed with both ends of the molecule to the electrodes. The majority of the chemisorbed contacts are made by an Au–S bond on both sides of the molecule, but the Au–NH$_2$ bonded molecules [63] are within the same low resistance group.

The medium resistance group, indicated in figures 18(a) and (b) by the shaded area, is a collection of data from
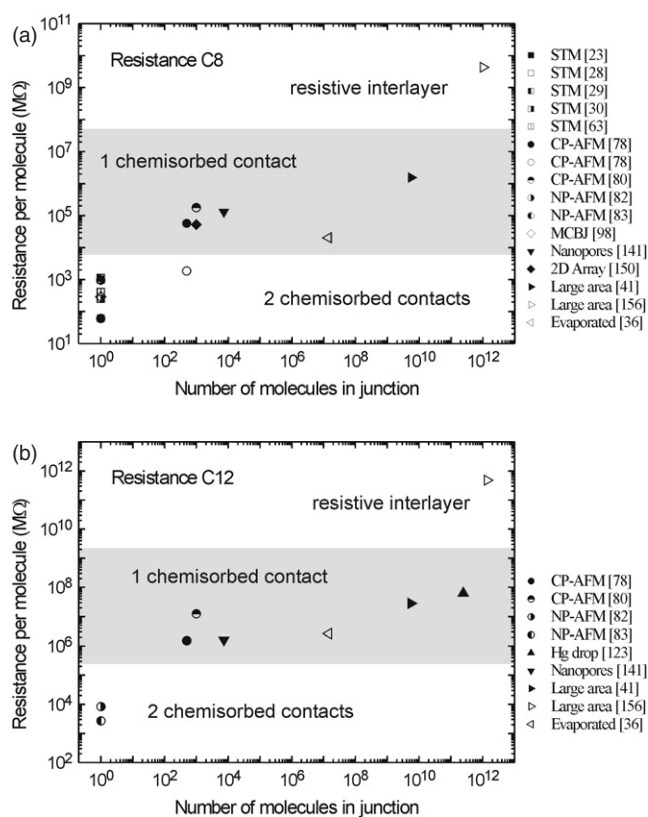
Figure 18. Resistance per molecule as a function of the number of molecules in the junction. (a) Obtained results with alkane-based molecules containing 8 carbons in the backbone. (b) Results obtained on molecules containing 12 carbon atoms in the alkane chain. For C8 as well as C12, a clear division in resistance is observed, solely due to the nature of the contacts.

experiments consisting of molecular junctions with one chemisorbed contact and one physisorbed contact. A SAM is chemisorbed on a bottom electrode and further in the process a top electrode is applied to the SAM by various techniques to create a physisorbed contact. Although the medium resistance group is clearly one collection of results, the number of molecules measured in the experimental molecular junctions range from 100 molecules up to 10^{11} molecules, encompassing nine orders of magnitude. If the increase in resistance per molecule with increasing device area would be due to physical effects, as previously suggested by Selzer *et al*, who reported a change in the conduction per molecule of several orders of magnitude due to presence or absence of neighboring molecules [32], there would be a significant shift in resistance within this medium resistance group. Due to the absence of such large differences in resistance within this group, it can be concluded that large differences between experiments originate solely from a difference in contacts. However, we can expect an increase in contact resistance with increasing device area from the general fact that the possibility for short circuit formation increases with increasing device area. In order to avoid short circuits in large area devices, the interaction between the applied top contact and the monolayer has to be less intimate (more gentle) for larger devices areas compared to small area devices, since the probability for short circuit

formation is less likely in a small area due to a pinhole free SAM. A weaker and moderate physisorbed contact leads to an increase in contact resistance or a decrease in transmission probability at the molecule/electrode interface, compared to a chemisorbed contact [23, 48, 49].

Alkanedithiol molecules were measured in large area molecular junctions [11, 31, 41], but since PEDOT:PSS is also weakly bound to thiol end groups, these molecular junctions cannot be regarded as junctions with chemisorbed contacts at both ends of the molecules and are, therefore, within the medium resistance group.

The high resistance group in figure 17 has an average contact resistance (R_0) of 6.1×10^6 MΩ per molecule in the junction. This high contact resistance can be explained by the presence of a second insulating layer or a high resistive interlayer in the junction. Shimizu *et al* use the PALO technique to fabricate Au electrodes on a SAM [163]. They use fatty acids, $CH_3(CH2)_{n-2}COOH$, to form monolayers on Al_2O_3. The insulating Al_2O_3 layer thickness was assumed to be 3 nm thick. Therefore, the total junction configuration consist of two tunnel barriers in series and this will result in a high contact resistance when the Al_2O_3 layer is regarded as part of the contacts, i.e., when the reported resistance per molecule is studied exclusively as a function of the alkane length (see figures 15 and 17). The other data of the high resistance group is by Milani *et al*, who spin coated a layer of PmPV with a thickness of 80 nm on top of a SAM [156]. They showed that the current flows only through the polymer region contacted by the hanging mercury drop top electrode. Similar to the PALO experiment, the PmPV layer is regarded as part of the contacts when the resistance per molecule is investigated as a function of the alkanethiol length of the SAM. The conductivity of a pure PmPV film was determined to be 2×10^{-12} S cm^{-1} [165]. Due to the low conductivity of the PmPV top layer, the total resistance of the molecular junction will be increased. This also explains the large difference observed, despite similar Au/SAM/polymer structure, between this technique and the other reported large area molecular junction experiments [11, 31, 41]. The latter contained a PEDOT:PSS layer with a conduction of ~20 S cm^{-1} on top of the SAM. Due to this high conduction of the PEDOT:PSS, similar resistances were obtained as in the CP-AFM experiments on monothiols and hanging mercury drop experiments, with the Hg drop directly in physical contact with the SAM.

5. Summary and perspective

We subdivided a general molecular junction into different components to determine their influence on the absolute values obtained for the resistance of alkane-based molecules and to determine their influence on the quality of the measurements. We described in detail the advantages and disadvantages of different techniques to measure the electronic transport through single molecules or self-assembled monolayers. When scaled to a single molecule, 8 orders of magnitude difference in conduction was found for C8 and C12 molecules. The obtained resistance per molecule (R_{mol}) was plotted versus

the number of carbon atoms present in the alkane chain, which resulted in three larger clusters of data compiled from different experimental testbeds. The low resistance group consists of STM and CP-AFM measurements, with alkanedithiol molecules chemically bonded to both electrodes, resulting in a low contact resistance. The medium resistance group consists of measurements on larger device areas with only one end of the molecule chemisorbed at an electrode. The other end is physically bound to the other electrode, resulting in the possibility to measure larger device areas without the formation of short circuits, but with a higher contact resistance compared to the low resistance group. The third collection of reported data demonstrates a high contact resistance, which is most likely due to the presence of an extra tunneling barrier or a poorly conducting layer in the molecular junction. All reports show a similar exponential increase of resistance with increasing alkane chain length, independent of the technology used. The obtained decay constants (β_N) range from 0.51 to 1.16, with an average value of 0.92 ± 0.19 per carbon from all experiments. Similar values of β_N are obtained in completely different device structures and device sizes, indicating that the decay constant β_N of alkane chains is ~0.9 per carbon, irrespective of the experimental testbed used to measure the electrical properties of alkane-based molecules.

What is the best technique to study the electrical properties of molecules? This is a question without a true answer. Since all recently reported molecular junctions consisting of alkane-based molecules result in a similar trend of an exponential increasing resistance with increasing molecule length, we have to conclude that proper measurements are done, irrespective of the configuration of the molecular junction. The same holds for the conductance of a single molecule. A different technique leads to a change in the absolute value of the conduction of a (single) molecule, due to a different nature of the contacts. Therefore, the conduction of a molecule can only be quantified with respect to the molecular junction used. This makes alkane(di)thiol molecules even more important as *the* reference system for any new technology related to molecular electronics. For benchmarking the technology, two electrical measurements have to be performed: (a) the length dependence of alkane-based molecules on the tunnel current, and (b) temperature dependence of the $I-V$ characteristics. Only then, the tunneling mechanism of the electrical transport through the molecules can be established. This will exclude the possibility of electrical properties observed due to electrodes, metal filaments or interface effects, which might otherwise be attributed to the properties of the molecules in the junctions. Furthermore, when the end group and the backbone of a molecule under study are varied at the same instant, it is impossible to attribute the change in conduction solely to the change in conjugation, packing, tilt angle or any other effect arising from a change of molecular backbone. The change in conduction due to a change of contact to the electrodes by changing the end group of the molecule can easily be a few orders of magnitude and needs to be taken into account. The decision of what technique to use in molecular electronics will thus depend on the motivations for the work. Fundamental studies might be best represented by single molecule techniques from the low resistance group, whereas application oriented research is more promising with reproducible techniques from the medium resistance group. Macroscopic devices based on a single molecular layer can be realized by using one of the techniques from the high resistance group and might lead to interesting low end applications. All techniques, when pursued, will for sure lead to more interesting and promising new results in the field of molecular electronics.

Acknowledgments

References

[1] Herwald S W and Angello S J 1960 Integration of circuit functions into solids *Science* **132** 1127

[2] Moore G E 1965 Cramming more components onto integrated circuits *Electronics* **38** 8

[3] Aviram A and Ratner M A 1974 Molecular rectifiers *Chem. Phys. Lett.* **29** 277

[4] Mann B and Kuhn H 1971 Tunneling through fatty acid salt monolayers *J. Appl. Phys.* **42** 4398

[5] Data obtained from ISI Web of Knowledge http://www.isiknowledge.com

[6] Porter M D, Bright T B, Allara D L and Chidsey C E D 1987 Spontaneously organized molecular assemblies. 4. structural characterization of *n*-alkyl thiol monolayers on gold by optical ellipsometry, infrared spectroscopy, and electrochemistry *J. Am. Chem. Soc.* **109** 3559

[7] Love J C, Estroff L A, Kriebel J K, Nuzzo R G and Whitesides G M 2005 Self-assembled monolayers of thiolates on metals as a form of nanotechnology *Chem. Rev.* **105** 1103

[8] Vericat C, Vela M E, Benitez G A, Gago J A M, Torrelles X and Salvarezza R C 2006 Surface characterization of sulfur and alkanethiol self-assembled monolayers on Au(111) *J. Phys.: Condens. Matter* **18** R867

[9] Tomfohr J K and Sankey O F 2002 Complex band structure, decay lengths, and Fermi level alignment in simple molecular electronic systems *Phys. Rev. B* **65** 245105

[10] Salomon A, Cahen D, Lindsay S. Tomfohr J, Engelkes V B and Frisbie C D 2003 Comparison of electronic transport measurements on organic molecules *Adv. Mater.* **15** 1881

[11] Akkerman H B, Blom P W M, de Leeuw D M and de Boer B 2006 Towards molecular electronics with large-area molecular junctions *Nature* **441** 69

[12] Chen F, Hihath J, Huang Z, Li X and Tao N J 2007 Measurement of single-molecule conductance *Annu. Rev. Phys. Chem.* **58** 535

[13] Lindsay S M and Ratner M A 2007 Molecular transport junctions: clearing mists *Adv. Mater.* **19** 23

[14] Tao N J 2006 Electron transport in molecular junctions *Nat. Nanotechnol.* **1** 173

[15] Solomon G C, Gagliardi A, Pecchia A, Frauenheim T, Di Carlo A, Reimers J R and Hush N S 2006 Understanding the ineleastic electron-tunneling spectra of alkanedithiols on gold *J. Chem. Phys.* **124** 094704

[16] Laibinis P E, Whitesides G M, Allara D L, Tao Y T, Parikh A N and Nuzzo R G 1991 Comparison of the structures and wetting properties of self-assembled

monolayers of *n*-alkanethiol on the coinage metal surfaces, Cu, Ag, Au *J. Am. Chem. Soc.* **113** 7152

[17] Zhitenev N B and Bao Z 2004 Single-and multigrain nanojunctions with a self-assembled monolayer of conjugated molecules *Phys. Rev. Lett.* **92** 186805

[18] Lee M H, Speyer G and Sankey O F 2006 Electron transport through single alkane molecules with different contact geometries on gold *Phys. Status Solidi* b **243** 2021

[19] Weiss E A, Chiechi R C, Kaufman G K, Kriebel J K, Li Z, Duati M, Rampi M A and Whitesides G M 2007 Influence of defects on the electrical characteristics of mercury-drop junctions: self-assembled monolayers of *n*-alkanethiolates on rough and smooth silver *J. Am. Chem. Soc.* **129** 4336

[20] Grigoriev A, Sköldberg J, Wendin G and Crljen Ž 2006 Critical roles of metal–molecule contacts in electron transport through molecular-wire junctions *Phys. Rev.* B **74** 045401

[21] Basch H, Cohen R and Ratner M A 2005 Interface geometry and molecular junction conductance: geometric fluctuation and stochastic switching *Nano Lett.* **5** 1668

[22] Losic D, Shapter J G and Gooding J J 2001 Influence of surface topography on alkanethiol SAMs assembled from solution and by microcontact printing *Langmuir* **17** 3307

[23] Xu B and Tao N J 2003 Measurement of single-molecule resistance by repeated formation of molecular junctions *Science* **301** 1221

[24] Hallbäck A S, Oncel N, Huskens J, Zandvliet H J W and Poelsema B 2004 Inelastic electron tunneling spectroscopy on decanethiol at elevated temperatures *Nano Lett.* **4** 1393

[25] Cui X D, Primak A, Zarate X, Tomfohr J, Sankey O F, Moore A L, Moore T A, Gust D, Harris G and Lindsay S M 2001 Reproducible measurement of single-molecule conductivity *Science* **294** 571

[26] Huang Z, Xu B, Chen Y, Di Ventra M and Tao N 2006 Measurement of current-induced local heating in a single molecule junction *Nano Lett.* **6** 1240

[27] Lörtscher E, Weber H B and Riel H 2007 Statistical approach to investigating transport through single molecules *Phys. Rev. Lett.* **98** 176807

[28] Suzuki M, Fujii S and Fujihira M 2006 Measurements of currents through single molecules of alkanedithiols by repeated formation of break junction in scanning tunneling microscopy under ultrahigh vacuum *Japan. J. Appl. Phys.* **45** 2041

[29] Haiss W, Nichols R J, van Zalinge H, Higgins S J, Bethell D and Schiffrin D J 2004 Measurement of single molecule conductivity using spontaneous formation of molecular wires *Phys. Chem. Chem. Phys.* **6** 4330

[30] Chen F, Li X, Hihath J, Huang Z and Tao N 2006 Effect of anchoring groups on single-molecule conductance: comparative study of thiol-, amine, and carboxylic-acid-terminated molecules *J. Am. Chem. Soc.* **128** 15874

[31] Akkerman H B, Naber R C G, Jongbloed B, van Hal P A, Blom P W M, de Leeuw D M and de Boer B 2007 Electron tunneling through alkanedithiol self-assembled monolayers in large-area molecular junctions *Proc. Natl Acad. Sci. USA* **104** 11161

[32] Selzer Y, Cai L, Cabassi M A, Yao Y, Tour J M, Mayer T S and Allara D L 2005 Effect of local environment on molecular conduction: isolated molecule versus self-assembled monolayer *Nano Lett.* **5** 61

[33] de Boer B, Frank M M, Chabal Y J, Jiang W, Garfunkel E and Bao Z 2004 Metallic contact formation for molecular electronics: interactions between vapor-deposited metals and self-assembled monolayers of conjugated mono- and dithiols *Langmuir* **20** 1539

[34] Haick H, Ghabboun J and Cahen D 2005 Pd versus Au as evaporated metal contacts to molecules *Appl. Phys. Lett.* **86** 042113

[35] Haynie B C, Walke A V, Tighe T B, Allara D and Winograd N 2003 Adventures in molecular electronics: how to attach wires to molecules *Appl. Surf. Sci.* **203/204** 433

[36] Kim T W, Wang G, Lee H and Lee T 2007 Statistical analysis of electronic properties of alkanethiols in metal–molecule–metal junctions *Nanotechnology* **18** 315204

[37] Ulman A 1996 Formation and structure of self-assembled monolayers *Chem. Rev.* **96** 1533

[38] Schreiber F 2000 Structure and growth of self-assembling monolayers *Prog. Surf. Sci.* **65** 151

[39] Leung T Y B, Gerstenberg M C, Lavrich D J and Scoles G 2000 1,6-hexanedithiol monolayers on Au(111): a multi-technique structural study *Langmuir* **16** 549

[40] Kohale S, Molina S M, Weeks B L, Khare R and Hope-Weeks L J 2007 Monitoring the formation of self-assembled monolayers of alkanedithiols using a micromechanical cantilever sensor *Langmuir* **23** 1258

[41] Akkerman H B, Kronemeijer A J, van Hal P A, de Leeuw D M, Blom P W M and de Boer B 2007 *Small* at press

[42] Dannenberger O, Buck M and Grunze M 1999 Self-Assembly of *n*-alkanethiols: a kinetic study by second harmonic generation *J. Phys. Chem.* B **103** 2202

[43] Krapchetov D A, Ma H, Jen A K Y, Fischer D A and Loo Y L 2005 Solvent-dependent assembly of therphenyl- and quarterphenyldithiol on gold and gallium arsenide *Langmuir* **21** 5887

[44] Asadi K, Gholamrezaie F, Smits E C P, Blom P W M and de Boer B 2007 Manipulation of charge carrier injection into organic field-effect transistors by self-assembled monolayers of alkanethiols *J. Mater. Chem.* **17** 1947

[45] Tour J M, Jones L II, Pearson D L, Lamba J J S, Burgin T P, Whitesides G M, Allara D L, Parikh A N and Atre S V 1995 Self-assembled monolayers and multilayers of conjugated thiols, α, ω-dithiols, and thioacetyl-containing adsorbates. Understanding attachments between potential molecular wires and gold surfaces *J. Am. Chem. Soc.* **117** 9529

[46] Maksymovych P, Sorescu D C and Yates J T Jr 2006 Gold-adatom mediated bonding in self-assembled short-chain alkanethiolate species on the Au(111) surface *Phys. Rev. Lett.* **97** 146103

[47] Vuillaume D and Lenfant S 2003 The metal/organic monolayer interface in molecular electronic devices *Microelectron. Eng.* **70** 539

[48] Kaun C C and Guo H 2003 Resistance of alkanethiol molecular wires *Nano Lett.* **3** 1521

[49] Seminario J M and Yan L 2005 *Ab initio* analysis of electron currents in thioalkanes *J. Quant. Chem.* **102** 711

[50] Imry Y and Landauer R 1999 Conductance viewed as transmission *Rev. Mod. Phys.* **71** 306

[51] Mujica V, Nitzan A, Datta S, Ratner M A and Kubiak C P 2003 Molecular wire junctions: tuning the conductance *J. Phys. Chem.* B **107** 91

[52] Zhu X Y 2004 Charge transport at metal–molecule interfaces: a spectroscopic view *J. Phys. Chem.* B **108** 8778

[53] Fujihira M, Suzuki M, Fujii S and Nishikawa A 2006 Currents through single molecular junction of Au/hexanedithiolate/Au measured by repeated formation of break junction in STM under UHV: effects of conformational change in an alkylene chain from *gauche* to *trans* and binding sites of thiolates on gold *Phys. Chem. Chem. Phys.* **8** 3876

[54] Binnig G, Rohrer H, Gerber Ch and Weibel E 1982 Tunneling through a controllable vacuum gap *Appl. Phys. Lett.* **40** 1982

[55] Li W, Virtanen A and Penner R M 1994 Self-Assembly of
     n-alkanethiolate monolayers on silver nanostructures:
     determination of the apparent thickness of the monolayer
     J. Phys. Chem. **98** 11751

[56] Yang Y C, Lee Y L, Yang L Y O and Yau S L 2006 *In situ*
     scanning tunneling microscopy of 1,6-hexadecanedithiol,
     1,9-nonanedithiol, 1,2-benzenedithiol, and
     1,3-benzenedithiol adsorbed on Pt(111) electrodes
     Langmuir **22** 5189

[57] Mendoza S M, Arfaoui I, Zanarini S, Paolucci F and
     Rudolf P 2007 Improvements in the characterization of the
     crystalline structure of acid-terminated alkanethiol
     self-assembled monolayers on au(111) *Langmuir* **23** 582

[58] Yang G and Liu G 2003 New insights for self-assembled
     monolayers of organothiols on Au(111) revealed by
     scanning tunneling microscopy *J. Phys. Chem.* B
     107 8746

[59] Zhang H M, Xie Z X, Mao B W and Xu X 2004
     Self-assembly of normal alkanes on the Au(111) surfaces
     Chem. Eur. J **10** 1415

[60] Qian Y, Yang G, Yu J, Jung T A and Liu G 2003 Structures of
     annealed decanethiol self-assembled monolayers on
     Au(111): an ultrahigh vacuum scanning tunneling
     microscopy study *Langmuir* **19** 6056

[61] Ito E, Konno K, Noh J, Kanai K, Ouchi Y, Seki K and
     Hara M 2005 Chain length dependence of adsorption
     structure of COOH-terminated alkanethiol SAMs on
     Au(111) *Appl. Surf. Sci.* **244** 584

[62] Esplandiu M J, Carot M L, Cometto F P, Macagno V A and
     Patrito E M 2006 Electrochemical STM investigation of
     1,8-octanedithiol monolayers on Au(111). Experimental
     and theoretical study *Surf. Sci.* **600** 155

[63] Venkataraman L, Klare J E, Tam I W, Nuckolls C,
     Hybertsen M S and Steigerwald M L 2006 Single-molecule
     circuits with well-defined molecular conductance *Nano
     Lett.* **6** 458

[64] Cygan M T *et al* 1998 Insertion, conductivity and structures of
     conjugated organic oligomers in self-assembled alkanethiol
     monolayers on Au(111) *J. Am. Chem. Soc.* **120** 2721

[65] Wakamatsu S, Akiba U and Fujihira M 2002 Electron
     tunneling through a single molecule embedded in
     self-assembled monolayer matrices *Colloids Surf.* A
     198–200 785

[66] Hallbäck A S, Poelsema B and Zandvliet H J W 2007
     Dynamics or stochastic conductance switching of
     phenylene–ethylene oligomers *ChemPhysChem* **8** 661

[67] McCarley R L, Dunaway D J and Willicut R J 1993 Mobility
     of the alkanethiol-gold(111) interface studied by scanning
     probe microscopy *Langmuir* **9** 2775

[68] Nishida N, Hara M, Sasabe H and Knoll W 1997 Formation
     and exchange processes of alkanethiol self-assembled
     monolayer on Au(111) studied by thermal desorption
     spectroscopy and scanning tunneling microscopy *Japan. J.
     Appl. Phys.* **36** 2379

[69] Woo D H, Choi E M, Yoon Y H, Kim K J, Jeon I C and
     Kang H 2007 Current–distance–voltage characteristics of
     electron tunneling through an electrochemical STM
     junction *Surf. Sci.* **601** 1554

[70] Rost M J *et al* 2005 Scanning probe microscopes go video rate
     and beyond *Rev. Sci. Instrum.* **76** 053710

[71] Binnig G, Quate C F and Gerber Ch 1986 Atomic force
     microscope *Phys. Rev. Lett.* **56** 930

[72] Wold J D and Frisbie C D 2000 Formation of
     metal–molecule–metal junctions: microcontacts to
     alkanethiol monolayers with a conducting AFM tip *J. Am.
     Chem. Soc.* **122** 2970

[73] van Duren J K J, Yang X, Loos J, Bulle-Lieuwema C W T,
     Sieval A B, Hummelen J C and Janssen R 2004 Relating
     the morphology of poly(*p*-phenylene

     vinylene)/methanofullerene blends to solar-cell
     performance *Adv. Funct. Mater.* **14** 425

[74] Mitzi D B, Kosbar L L, Murray C E, Copel M and
     Afzali A 2004 High-mobility ultrathin semiconducting
     films prepared by spincoating *Nature* **428** 299

[75] Naber R C G, de Boer B, Blom P W M and
     de Leeuw D M 2005 Low-voltage polymer field-effect
     transistors for nonvolatile memories *Appl. Phys. Lett.*
     87 203509

[76] Komura M and Iyoda T 2007 AFM cross-sectional imaging of
     perpendicularly oriented nanocylinder structures of
     microphase-separated block copolymer films by
     crystal-like cleavage *Macromol.* **40** 4106

[77] Li X, He J, Hihath J, Xu B, Lindsay S M and Tao N 2006
     Conductance of single alkanedithiols: conduction
     mechanism and effect of molecule–electrode contacts
     J. Am. Chem. Soc. **128** 2135

[78] Engelkes V B, Beebe J M and Frisbie C D 2004
     Length-dependent transport in molecular junctions based
     on SAMS of alkanethiols and alkanedithiols: effect of
     metal work function and applied bias on tunneling
     efficiency and contact resistance *J. Am. Chem. Soc.*
     126 14287

[79] Sakaguchi H, Hirai A, Iwata F, Sasaki A, Nagamura T,
     Kawata E and Nakabayashi S 2001 Determination of
     performance on tunnel conduction through molecular wire
     using a conductive atomic force microscope *Appl. Phys.
     Lett.* **79** 3708

[80] Beebe J M, Engelkes V B, Miller L L and Frisbie C D 2002
     Contact resistance in metal–molecule–metal junctions
     based on aliphatic SAMs: effects of surface linker and
     metal work function *J. Am. Chem. Soc.* **124** 11268

[81] Engelkes V B, Beebe J M and Frisbie C D 2005 Analysis of
     the causes of variance in resistance measurements on
     metal–molecule–metal junctions formed by
     conducting-probe atomic force microscopy *J. Phys. Chem.*
     B **109** 16801

[82] Cui X D, Primak A, Zarate X, Tomfohr J, Sankey O F,
     Moore A L, Moore T A, Gust D, Nagahara L A and
     Lindsay S M 2002 Changes in the electronic properties of a
     molecule when it is wired into a circuit *J. Phys. Chem.* B
     106 8609

[83] Morita T and Lindsay S 2007 Determination of single
     molecule conductances of alkanedithiols by
     conducting-atomic force microscopy with large gold
     nanoparticles *J. Am. Chem. Soc.* **129** 7262

[84] Song H, Lee H and Lee T 2007 Intermolecular chain-to-chain
     tunneling in metal–alkanethiol–metal junctions *J. Am.
     Chem. Soc.* **129** 3806

[85] Humphris A D L, Miles M J and Hobbs J K 2005 A
     mechanical microscope: high-speed atomic force
     microscope *Appl. Phys. Lett.* **86** 034106

[86] Muller C J, van Ruitenbeek J M and de Jongh L J 1992
     Experimental observation of the transition from weak link
     to tunnel junction *Physica* C **191** 485

[87] Moreland J and Ekin J W 1985 Electron tunneling
     experiments using Nb–Sn 'break' junctions *J. Appl. Phys.*
     58 3888

[88] Agraït N, Yeyati A L and van Ruitenbeek J M 2003
     Quantum properties of atomic-sized conductors *Phys. Rep.*
     377 81

[89] van Ruitenbeek J M, Alvarez A, Piñero I, Grahmann C,
     Joyez P, Devoret H, Esteve D and Urbina C 1995
     Adjustable nanofabricated atomic size contacts *Rev. Sci.
     Instrum.* **67** 108

[90] Vrouwe S A G, van der Giessen E, van der Molen S J,
     Dulic D, Trouwborst M L and van Wees B J 2005
     Mechanics of lithographically defined break junctions
     Phys. Rev. B **71** 035313

[91] Reed M A, Zhou C, Muller C J, Burgin T P and Tour J M 1997 Conductance of a molecular junction *Science* **278** 252

[92] Krans J M, Muller C J, Yanson I K, Govaert Th C M, Hesper R and van Ruitenbeek J M 1993 One-atom point contacts *Phys. Rev.* B **48** 14721

[93] Lagos M, Rodrigues V and Ugarte D 2007 Structural and electronic properties of atomic-size wires at low temperatures *J. Electron Spectrosc. Relat. Phenom.* **156–158** 20

[94] Kergueris C, Bourgoin J P, Palacin S, Esteve D, Urbina C, Magoga M and Joachim C 1999 Electron transport through a metal–molecule–metal junction *Phys. Rev.* B **59** 19

[95] Dulic D, van der Molen S J, Kudernac T, Jonkman H T, de Jong J J D, Bowden T N, van Esch J, Feringa B L and van Wees B J 2003 One-way optoelectronic switching of photochromic molecules on gold *Phys. Rev. Lett.* **91** 207402

[96] Smit R H M, Noat Y, Untiedt C, Lang N D, van Hemert M C and van Ruitenbeek J M 2002 Measurement of the conductance of a hydrogen molecule *Nature* **419** 906

[97] Nielsen S K, Brandbyge M, Hansen K, Stokbro K, van Ruitenbeek J M and Besenbacher F 2002 Current–voltage curves of atomic-sized transition metal contacts: an explanation of why Au is ohmic and Pt is not *Phys. Rev. Lett.* **89** 066804

[98] González M T, Wu S, Huber R, van der Molen S J, Schönenberger C and Calame M 2006 Electrical conductance of molecular junctions by a robust statistical analysis *Nano Lett.* **6** 2238

[99] Fernandéz-Seivane L, García-Suárez V M and Ferrer J 2007 Predictions for the formation of atomic chains in mechanically controllable break-junction experiments *Phys. Rev.* B **75** 075415

[100] Romaner L, Heimel G, Gruber M, Brédas J L and Zojer E 2006 Stretching and breaking of a molecular junction *Small* **2** 1468

[101] Park H, Lim A K L, Alivisatos A P, Park J and McEuen P L 1999 Fabrication of metallic electrodes with nanometer separation by electromigration *Appl. Phys. Lett.* **75** 301

[102] Noguchi Y, Nagase T, Kubota T, Kamikado T and Mashiko S 2006 Fabrication of Au–molecule–Au junctions using electromigration method *Thin Solid Films* **499** 90

[103] Park J *et al* 2002 Coulomb blockade and the Kondo effect in single-atom transistors *Nature* **417** 722

[104] Liang W, Shores M P, Bockrath M, Long J R and Park H 2002 Kondo resonance in a single-molecule transistor *Nature* **417** 725

[105] Sordan R, Balasubramanian K, Burghard M and Kern K 2005 Coulomb blockade phenomena in electromigration break junctions *Appl. Phys. Lett.* **87** 013106

[106] Ghosh S, Halimun H, Mahapatro A K, Choi J, Lodha S and Janes D 2005 Device structure for electronic transport through individual molecules using nanoelectrodes *Appl. Phys. Lett.* **87** 233509

[107] Heersche H B, Lientschnig G, O'Neill K, van der Zant H S J and Zandbergen H W 2007 *In situ* imaging of electromigration-induced nanogap formation by transmission electron microscopy *Appl. Phys. Lett.* **91** 072107

[108] Trouwborst M L, van der Molen S J and van Wees B J 2006 The role of Joule heating in the formation of nanogaps by electromigration *J. Appl. Phys.* **99** 114316

[109] Loo Y L, Willett R L, Baldwin K W and Rogers J A 2002 Additive, nanoscale patterning of metal films with a stamp and a surface chemistry mediated transfer process: applications in plastic electronics *Appl. Phys. Lett.* **81** 562

[110] Kumar A and Whitesides G M 1993 Features of gold having micrometer to centimeter dimensions can be formed through a combination of stamping with an elastomeric stamp and an alkanethiol 'ink' followed by chemical etching *Appl. Phys. Lett.* **63** 2002

[111] Kumar A, Biebuyck H A and Whitesides G M 1994 Patterning self-assembled monolayers: applications in material science *Langmuir* **10** 1498

[112] Xia Y and Whitesides G M 1998 Soft lithography *Angew. Chem. Int. Edn* **37** 550

[113] Balmer T E, Schmid H, Stutz R, Delamarche E, Michel B, Spencer N D and Wolf H 2005 Diffusion of alkanedithiols in PDMS and its implications on microcontact printing (μ CP) *Langmuir* **21** 622

[114] Gates B D, Stewart M, Ryan D, Willson C G and Whitesides G M 2005 New approaches to nanofabrication: molding, printing, and other techniques *Chem. Rev.* **105** 1171

[115] Loo Y L, Willet R L, Baldwin K W and Rogers J A 2002 Interfacial chemistries for nanoscale transfer printing *J. Am. Chem. Soc.* **124** 7654

[116] Hsu J W P, Lang D V, West K W, Loo Y L, Halls M D and Raghavachari K 2005 Probing occupied states of the molecular layer in Au–Alkanedithiol–GaAs diodes *J. Phys. Chem.* B **109** 5719

[117] Loo Y L, Lang D V, Rogers J A and Hsu J W P 2003 Electrical contacts to molecular layers by nanotransfer printing *Nano Lett.* **3** 913

[118] Becucci L, Moncelli M R and Guidelli R 1996 Surface charge density measurements on mercury electrodes covered by phospholipid monolayers *J. Electroanal. Chem.* **413** 187

[119] Slowinski K, Chamberlain R V, Miller C J and Majda M 1997 Through-bond and chain-to-chain coupling. Two pathways in electron tunneling through liquid alkanethiol monolayers on mercury electrodes *J. Am. Chem. Soc.* **119** 11910

[120] Rampi M A, Schueller O J A and Whitesides G M 1998 Alkanethiol self-assembled monolayers as the dielectric of capacitors with nanoscale thickness *Appl. Phys. Lett.* **72** 1781

[121] Haag R, Rampi M A, Holmlin R E and Whitesides G M 1999 Electrical breakdown of aliphatic and aromatic self-assembled monolayers used as nanometer-thick organic dielectrics *J. Am. Chem. Soc.* **121** 7895

[122] Slowinski K, Fong H K Y and Majda M 1999 Mercury–mercury tunneling junctions. 1. Electron tunneling across symmetric and asymmetric alkanethiolate bilayers *J. Am. Chem. Soc.* **121** 7257

[123] York R L, Nguyen P T and Slowinski K 2003 Long-range electron transfer through monolayers and bilayers of alkanethiols in electrochemically controlled Hg–Hg tunneling junctions *J. Am. Chem. Soc.* **125** 5948

[124] Tran E, Duati M, Ferri V, Müllen K, Zharnikov M, Whitesides G M and Rampi M A 2006 Experimental approaches for controlling current flowing through metal–molecule–metal junctions *Adv. Mater.* **18** 1323

[125] Rampi M A and Whitesides G M 2002 A versatile experimental approach for understanding electron transport through organic molecules *Chem. Phys.* **281** 373

[126] Sek S, Bilewicz R and Slowinski K 2004 Electrochemical wiring of α, ω-alkanedithiol molecules into an electrical circuit *Chem. Commun.* 404

[127] Duatti M *et al* 2006 Electron transport across hexa-*peri* hexabenzocoronene units in a metal–self-assembled monolayer–metal junction *Adv. Mater.* **18** 329

[128] Holmlin R E, Haag R, Chabinyc M L, Ismagilov R F, Cohen A E, Terfort A, Rampi M A and Whitesides G M 2001 Electron transport through thin organic films in metal–insulator–metal junctions based on self-assembled monolayers *J. Am. Chem. Soc.* **123** 5075

[129] Salomon A, Boecking T, Seitz O, Markus T, Amy F, Chan C, Zhao W, Cahen D and Kahn A 2007 *What is the Barrier for Tunneling Through Alkyl Monolayers? Results from n- and p-Si-Alkyl/Hg Junctions* vol 19, p 445

[130] Holmlin R E, Ismagilov R F, Haag R, Mujica V, Ratner M A, Rampi M A and Whitesides G M 2001 Correlating electron transport and molecular structure in organic thin films *Angew. Chem. Int. Edn* **40** 2316

[131] Watson C M, Dwyer D J, Andle J C, Bruce A E and Bruce M R M 1999 Stripping analysis of mercury using gold electrodes: irreversible adsorption of mercury *Anal. Chem.* **71** 3181

[132] Li J and Abruña H D 1997 Phases of underpotentially deposited Hg on Au(111): an *in situ* surface x-ray diffraction study *J. Phys. Chem.* B **101** 2907

[133] Vasjari M, Shirshov Y M, Samoylov A V and Mirsky V M 2007 SPR investigation of mercury reduction and oxidation on thin gold electrodes *J. Electroanal. Chem.* **605** 73

[134] Li J and Abruña H D 1997 Coadsorption of sulfate/bisulfate anions with Hg cations during Hg underpotential deposition on Au(111): an *in situ* x-ray diffraction study *J. Phys. Chem.* B **101** 244

[135] Grave C, Tran E, Samori P, Whitesides G M and Rampi M A 2004 Correlating electrical properties and molecular structure of SAMs organized between two metal surfaces *Synth. Met.* **147** 11

[136] Zhou C, Deshpande M R, Reed M A, Jones L II and Tour J M 1997 Nanoscale metal/self-assembled monolayer/metal heterostructures *Appl. Phys. Lett.* **71** 611

[137] Chen J, Reed M A, Rawlett A M and Tour J M 1999 Large on–off ratios and negative differential resistance in a molecular electronic device *Science* **286** 1550

[138] Wang W, Lee T, Kamdar M, Reed M A, Stewart M P, Hwang J J and Tour J M 2003 Electrical characterization of metal–molecule–silicon junctions *Superlatt. Microstruct.* **33** 217

[139] Majumdar N, Gergel N, Routenberg D, Bean J C, Harriott L R, Li B, Pu L, Yao Y and Tour J M 2005 Nanowell device for the electrical characterization of metal–molecule–metal junctions *J. Vac. Sci. Technol.* B **23** 1417

[140] Hwang G J, Jeng R P, Lien C, Chen C S, Tsao Y S, Hwang H S, Xu S Q, Hong T M and Chou Y C 2006 Field effects on electron conduction through self-assembled monolayers *Appl. Phys. Lett.* **89** 133120

[141] Wang W, Lee T and Reed M A 2003 Mechanism of electron conduction in self-assembled alkanethiol monolayer devices *Phys. Rev.* B **68** 035416

[142] Wang W, Lee T and Reed M A 2003 Electronic transport in self-assembled alkanethiol monolayers *Physica* E **19** 117

[143] Wang W, Lee T, Kretzschmar I and Reed M A 2004 Inelastic electron tunneling spectroscopy of an alkanedithiol self-assembled monolayer *Nano Lett.* **4** 643

[144] Kushmerick J G, Holt D B, Yang J C, Naciri J, Moore M H and Shashidhar R 2002 Metal–molecule contacts and charge transport across monomolecular layers: measurement and theory *Phys. Rev. Lett.* **89** 086802

[145] Kushmerick J G, Holt D B, Pollack S K, Ratner M A, Yang J C, Schull T L, Naciri J, Moore M H and Shashidhar R 2002 Effect of bond-length alternation in molecular wires *J. Am. Chem. Soc.* **124** 10654

[146] Kushmerick J G, Whitaker C M, Pollack S K, Schull T L and Shashidhar R 2004 Tuning current rectification across molecular junctions *Nanotechnology* **15** 489

[147] Beebe J M and Kushmerick J G 2007 Nanoscale switch elements from self-assembled monolayers on silver *Appl. Phys. Lett.* **90** 083117

[148] Kushmerick J G, Naciri J, Yang J C and Shashidhar R 2003 Conductance scaling of molecular wires in parallel *Nano Lett.* **3** 897

[149] Blum A S, Kushmerick J G, Pollack S K, Yang J C, Moore M, Naciri J, Shashidhar R and Ratna B R 2004 Charge transport and scaling in molecular wires *J. Phys. Chem.* B **108** 18124

[150] Liao J, Bernard L, Langer M, Schönenberger C and Calame M 2006 Reversible formation of molecular junctions in 2D nanoparticle arrays *Adv. Mater.* **18** 2444

[151] Huang S, Sakaue H, Shingubara S and Takahagi T 1998 Self-organization of a two-dimensional array of gold nanodots encapsulated by alkanethiol *Japan. J. Appl. Phys.* **37** 7198

[152] Huang S, Tsutsui G, Sakaue H, Shingubara S and Takahagi T 2001 Formation of a large-scale Langmuir–Blodgett monolayer of alkanethiol-encapsulated gold particles *J. Vac. Sci. Technol.* B **19** 115

[153] Huang S, Tsutsui G, Sakaue H, Shingubara S and Takahagi T 2001 Experimental conditions for a highly ordered monolayer of gold nanoparticles fabricated by the Langmuir–Blodgett method *J. Vac. Sci. Technol.* B **19** 2045

[154] Santhanam V, Liu J, Agarwal R and Andres R P 2003 Self-assembly of uniform monolayer arrays of nanoparticles *Langmuir* **19** 7881

[155] Nardes A M, Kemerink M, Janssen R A J, Bastiaansen J A M, Kiggen N M M, Langeveld B M W, van Breemen A J J M and de Kok M M 2007 Microscopic understanding of the anisotropic conductivity of PEDOT:PSS thin films *Adv. Mater.* **19** 1196

[156] Milani F, Grave C, Ferri V, Samori P and Rampi M A 2007 Ultrathin π-conjugated polymer films for simple fabrication of large-area molecular junctions *ChemPhysChem* **8** 515

[157] Amlani I, Rawlett A M, Nagahara L A and Tsui R K 2002 An approach to transport measurements of electronic molecules *Appl. Phys. Lett.* **80** 2761

[158] Bolotin K I, Kuemmeth F, Pasupathy A N and Ralph D C 2004 Metal–nanoparticle single-electron transistors fabricated using electromigration *Appl. Phys. Lett.* **84** 3154

[159] Chu C, Na J S and Parsons G N 2006 Conductivity in alkylamine/gold and alkanethiol/gold molecular junctions measured in molecule/nanoparticle/molecule bridges and conducting probe structures *J. Am. Chem. Soc.* **129** 2287

[160] Long D P, Patterson C H, Moore M H, Seferos D S, Bazan G and Kushmerick J G 2005 Magnetic directed assembly of molecular junctions *Appl. Phys. Lett.* **86** 153105

[161] Long D P *et al* 2006 Effects of hydration on molecular junction transport *Nat. Mater.* **5** 901

[162] Vilan A and Cahen D 2002 Soft contact deposition onto molecularly modified GaAs. Thin metal film flotation: principles and electrical effects *Adv. Funct. Mater.* **12** 795

[163] Shimizu K T, Fabbri J D, Jelincic J J and Melosh N A 2006 Soft deposition of large-area metal contacts for molecular electronics *Adv. Mater.* **18** 1499

[164] Xu T, Morris T A, Szulczewski G J, Metzger R M and Szablewski M 2002 Current–voltage characteristics of an LB monolayer of didecylammonium tricyanoquinodimethanide measured between macroscopic gold electrodes *J. Mater. Chem.* **12** 3167

[165] Coleman J N, Curran S, Dalton A B, Davey A P, McCarthy B, Blau W and Barklie R C 1998 Percolation-dominated conductivity in a conjugated-polymer–carbon-nanotube composite *Phys. Rev.* B **58** 7492